INFORMATION TO USERS

This manuscript has been reproduced from the microfilm master. UMI films the text directly from the original or copy submitted. Thus, some thesis and dissertation copies are in typewriter face, while others may be from any type of computer printer.

The quality of this reproduction is dependent upon the quality of the copy submitted. Broken or indistinct print, colored or poor quality illustrations and photographs, print bleedthrough, substandard margins, and improper alignment can adversely affect reproduction.

In the unlikely event that the author did not send UMI a complete manuscript and there are missing pages, these will be noted. Also, if unauthorized copyright material had to be removed, a note will indicate the deletion.

Oversize materials (e.g., maps, drawings, charts) are reproduced by sectioning the original, beginning at the upper left-hand corner and continuing from left to right in equal sections with small overlaps.

Photographs included in the original manuscript have been reproduced xerographically in this copy. Higher quality 6" x 9" black and white photographic prints are available for any photographs or illustrations appearing in this copy for an additional charge. Contact UMI directly to order.

ProQuest Information and Learning
300 North Zeeb Road, Ann Arbor, MI 48106-1346 USA
800-521-0600

UMI®

Université d'Ottawa · University of Ottawa

SIMULATION OF DEWATERING DURING CONSTRUCTION OF A BEDROCK TUNNEL, NEPEAN, ONTARIO

by

Brent Loney

A thesis submitted to the School of Graduate Studies and Research

in partial fulfillment of the requirements

for the degree of M.Sc. in Earth Sciences

OTTAWA-CARLETON GEOSCIENCE CENTRE

AND

UNIVERSITY OF OTTAWA

OTTAWA, CANADA

Abstract

This thesis presents the results of groundwater flow modeling completed to simulate the effects of construction dewatering during the advance of a bedrock tunnel through an aquifer that serves as the source of water for numerous adjacent domestic water wells. The modeling was retrospective and consequently a large amount of data collected during the course of the tunnel project was available for the purpose of model calibration. Actual drawdown levels due to tunnel dewatering resulted in a significant number of well interference problems.

The model was constructed through the application of standard groundwater flow modeling techniques using the United States Geological Survey's modular groundwater flow modeling program (MODFLOW), and was designed to provide a reasonable representation of the groundwater flow system within which the tunnel was constructed. The model simulated the tunnel as a drain which advances with time through the use of successive stress periods. While there were some deficiencies with the transient calibration, the overall calibrated solution was found to provide a sufficiently realistic simulation of the actual dewatering impacts observed to both validate the approach used and allow the use of the model for prediction.

The results of this study suggest that when evaluating tunnel dewatering impacts from a flow system perspective, it is not necessary to assess groundwater inflow at the tunnel face as a separate issue (as has been emphasized in other investigations, which approached the problem from more of an engineering perspective), or even to quantify it

at all. This stems from the fact that the tunnel acts as a drain and the tunnel advance rates are sufficiently slow that the drawdown response approaches steady state on a shorter time scale than both the advance of the tunnel and the subsequent installation of an impermeable liner. Consequently, even simulating the tunnel with a relatively small number of stress periods (i.e. simulating the tunnel advance as large segments per unit time) still yielded relatively good calibrations with respect to both simulated drawdown and flow rates.

An evaluation of grouting efforts that were undertaken to reduce the rate of groundwater inflow to the tunnel was completed by assuming that the effectiveness of this grouting program could be directly related to the contrast between the hydraulic conductivity of the aquifer ($K_{aquifer}$) and the hydraulic conductivity of the grouted rock immediately surrounding the tunnel (K_{drain}). With this in mind, the calibrated model used a value for K_{drain} which was 17 times lower than that of $K_{aquifer}$. The results of predictive simulations completed using the calibrated model showed that the tunnel's impact would have been substantially greater had no grouting efforts been completed (i.e. $K_{drain} = K_{aquifer}$).

The results of other predictive simulations showed that the rate of tunnel advance had no effect upon the level of impact observed and that it may have been feasible to minimize the number of well interference problems experienced through artificial aquifer recharge using injection wells.

Résumé

Cette thèse présente les résultats d'un modèle numérique simulant l'écoulement des eaux souterraines lorsque la nappe phréatique fut abaissée durant l'avancement d'un tunnel foré dans le roc au travers d'un aquifer servant comme source d'eau potable pour plusieurs puits domestiques adjacents. Le modèle numérique est rétrospectif et, par conséquent, une grande quantité de données prises durant le cours du projet ont pu être utilisées pour les fins de calibration. Les niveaux actuels de rabattement de la nappe phréatique occasionnée par le captage de l'eau souterraine, nécessaire à la construction du tunnel, a occasionné un nombre de problèmes d'interférence dans les puits existants.

Le modèle fut construit en appliquant des techniques standards pour l'écoulement des eaux souterraines, utilisant le "Modular Groundwater Flow Modeling Program" (MODFLOW) du "United States Geological Survey", et fut conçu afin de pourvoir une représentation raisonnable du système d'eau soûterraine dans laquelle le tunnel fut construit. Le modèle a simulé le tunnel comme un drain avancant dans le temps en se servant de périodes successives de stress. Tandis qu'il y eu certaines déficiences avec la calibration transitoire, la solution totale de la calibration a pourvu une simulation suffisament réaliste pour les impacts actuels occasionnés par le rabattement de la nappe phréatique, afin de valider l'approche utilisée et aussi afin de pouvoir se servir du modèle pour des fins de prédiction.

Les résultats de cette étude suggèrent que, lorsqu'on évalu les impacts de l'abaissement de la nappe phréatique durant la construction d'un tunnel, suivant la perspective du système total, il n'est pas nécessaire de déterminer le débit d'entée de l'eau souterraine à la façe du tunnel comme facteur séparé (contrairement à l'emphase placée sur la façe dans d'autres investigations qui ont approché le problème d'une perspective de génie) ou

même de quantifier ce débit. Ceci provient du fait que le tunnel agit comme drain et que la vitesse d'avancement du tunnel est suffisament faible que la réponse à l'abaissement de la nappe approche l'écoulement à l'état stable à une échelle de temps qui est moindre que l'avancement du tunnel et de l'installation subséquente de la chemise imperméable. Par conséquent, en simulant le tunnel avec un nombre relativement restraint de périodes de stress (c.-à-d. en simulant l'avancement du tunnel comme de grands segments par unité de temps) a produit des calibrations relativement bonnes pour le rabattement de la nappe phréatique et des débits.

Une évaluation des efforts d'injection de coulis qui ont été entreprises, afin de réduire le débit d'infiltration de l'eau souterraine dans le tunnel, a été complétée en présumant que l'efficacité de ce programme d'injection pouvait être directement relié au contraste entre la conductivité hydraulique de l'aquifère ($K_{aquifère}$) et la conductivité hydraulique du roc injecté avec le coulis autour du tunnel (K_{drain}). Avec ceci en tête, la calibration du modèle a utilisée une valeur de K_{drain} qui est 17 fois plus basse que celle de $K_{aquifère}$. Les résultats des simulations prédictives complétées utilisant le modèle calibré ont démontrés que l'impact du tunnel aurait été beaucoup plus grand si aucune injection de coulis n'avait été accomplie (c.-à-d. $K_{drain} = K_{aquifère}$).

Les résultats des simulations prédictives ont démontrés que la vitesse d'avancement du tunnel n'a pas eu d'effet sur le niveau d'impact observé et qu'il aurait été possible de minimiser le nombre de problèmes d'interférence des puits existants en utilisant des puits d'injection pour recharger l'aquifère.

TABLE OF CONTENTS

APPENDICES

LIST OF TABLES

LIST OF ILLUSTRATIONS

1.0 Introduction

This thesis describes the development of a groundwater flow model to simulate the effects of dewatering during the construction of a bedrock tunnel and presents the results of the various simulations calculated by the model code.

The modeling is retrospective in that the construction activity simulated was completed prior to the modeling effort, during 1994/95. Due to the fact that portions of the tunnel were completed within an urban area consisting of privately serviced residences (i.e. well and septic systems), the potential for well interference problems was recognized during the planning stages of the tunnel project. As such, numerous groundwater monitoring wells were constructed in the vicinity of the proposed tunnel prior to construction and these were monitored for a significant period of time before, during, and after the tunnel was completed. Consequently, a large database of groundwater monitoring data was available for this study. In addition, considerable data on dewatering (pumping) rates and locations (i.e. tunnel advance), local hydrogeological parameters, and local groundwater chemistry were also obtained during the course of the tunnel project. Furthermore, due to the nature of this type of construction project, direct observation of dewatering effects within the aquifer (i.e. within the tunnel) was possible. As a result, the sum total of data available was seen to present an invaluable opportunity for further study through the development of a groundwater flow model.

1.1 Objectives

In addition to allowing for a better understanding of the local groundwater flow regime, the primary objective of this study was to determine whether impacts to this groundwater regime due to tunneling could be effectively simulated using standard numerical groundwater flow modeling techniques. Specifically, the model was required to simulate transient effects due to dewatering during the advance of an open bedrock tunnel within a confined, fractured bedrock aquifer. Problems to be addressed included the selection of boundary conditions and the assignment of stress periods which would be adequately representative of the changing conditions (both spatial and temporal) associated with this type of construction dewatering. In addition, the development of this model would allow for a determination as to whether the use of an equivalent porous medium approach to the simulation of groundwater flow in fractured bedrock presented any significant limitations to this type of modeling application. Assuming adequate calibration (both steady state and transient), the model could then be utilized for running predictive simulations of hypothetical construction scenarios in order to provide a better understanding of the relationship between various construction methodologies and the resulting impact to the aquifer. A further objective of the study was to simulate geochemical impacts to the aquifer through the application of standard contaminant transport modeling techniques to the groundwater flow model.

With these objectives in mind, the modeling codes used for this study consisted of the widely used MODFLOW (McDonald and Harbaugh, 1988) for groundwater flow, and MT3D

(Zheng, 1990) for contaminant transport (further description and the basis for these selections is provided later in the thesis).

1.2 Previous Studies

A review of the available literature indicates that groundwater impacts associated with construction dewatering have generally been addressed from two distinct perspectives, which could be characterized as an engineering perspective, and a hydrogeological, or flow system, perspective. The latter category deals largely with dewatering impacts to the overall groundwater flow regime, whereas the former is more concerned with dewatering issues as an engineering or construction constraint (e.g. engineering design of dewatering systems, techniques to control groundwater inflow, etc.).

1.2.1 Engineering Perspective

From an engineering perspective, previous work related to dewatering associated with tunneling has focused on predicting groundwater inflows to the open tunnel excavation. Application of these techniques during the construction design stage would give engineers some indication as to the size and type of pumping systems required to maintain reasonably dry conditions within the excavation (so as to allow work to physically proceed), or provide an indication as to the type of controls which may be required to limit groundwater inflow to the excavation (e.g. grouting, installation of low permeability liners).

Goodman et al. (1965) provide a widely used analytical technique for predicting the rate of groundwater inflow per unit length of tunnel (steady state case) or the rate of inflow at any

time *t* after the breakdown of steady flow (transient case). While extremely useful from an engineering perspective, the technique is nevertheless limited due to its requirement of a fairly restrictive set of assumptions. Notably, the technique requires that the hydraulic head above the tunnel be known (or estimated) and thus is of limited use in terms of assessing impacts to the overall groundwater flow regime. The technique also assumes that the tunnel is driven into a water table (unconfined) aquifer and, in the transient case, that the water table represents a free surface discharging at a seepage face (the tunnel) and that the Dupuit-Forchheimer horizontal flow assumptions hold. Freeze and Cherry (1979) characterized the technique as follows: "(it) may be suitable for order-of-magnitude design inflow estimates, but it should be used with a healthy dose of skepticism". Section 1.3 gives an example of an application of this approach to predict tunnel dewatering impacts during design stage studies for this specific tunnel project (OMM, 1993a).

Numerical techniques have been utilized in order to provide a better prediction of the magnitude of transient inflows that could occur at the tunnel face (i.e. at the leading face of tunnel mining). One such method is described by Anagnostou (1995), wherein the transient inflow at the tunnel face and the resulting head distribution are calculated through application of a finite element solution. Again, the method assumes water table conditions with the water table representing a free surface. The advance of the tunnel with time is accounted for by solving for quasi-steady state conditions (steady state conditions with a moving frame of reference). The model is made computationally less complex through allowing the finite element mesh to advance with the tunnel face. This would present a significant limitation in

any attempt to apply this method to a flow system oriented approach, as other boundary conditions would be similarly affected. Furthermore, since inflow can only occur at the tunnel face, it is apparent that drawdown over the remainder of the tunnel alignment may be under-predicted.

In summary, the above described body of work has limited application to the problem at hand. This is generally due either to the requirement that fairly restrictive assumptions be made, or a focus weighted too heavily on impacts due to groundwater inflows at the tunnel face. This latter factor in particular would significantly hinder the application of these techniques to a problem focused more on the overall impact to the groundwater flow system.

1.2.2 Flow System Perspective

Numerous studies have approached construction dewatering problems from a flow system perspective. However, published accounts of these types of applications are primarily limited to different types of dewatering situations than the subject of this study. Good examples of these types of applications are provided by Toran and Bradbury (1988) and by Eberts and Bair (1990). Both of these studies consisted of applications of MODFLOW to predict the impacts to local groundwater flow regimes due to the cessation of long term dewatering (due to underground mine workings in the former case and open pit quarry operations in the latter). The authors in both cases were able to rely upon a significant amount of data relating to conditions before and during mining operations for model calibration. Both models were subsequently used to simulate the post-mining (i.e. recovered) conditions and allow an assessment of specific water quality issues that could arise.

The most important difference between these applications and this study lies in the fact that both of the above described investigations could justifiably model steady state dewatering conditions. The present study however, could not make such an assumption due to the relatively shorter period during which the mining works were open and the requirement to simulate dewatering effects in close proximity to the tunnel (i.e. spatial and temporal changes in the excavation are more significant).

Schweiger et al. (1993) describe a modeling investigation completed to predict the effects of dewatering during the construction of a proposed tunnel near a nature reserve. Although the authors' definition of the problem is scant, it is evident that there were concerns related to potential lowering of the shallow water table in the area and the effects this could have on mineral springs within the nature reserve. Consequently, this situation is conceptually similar to that described by the present study. The approach used by the authors generally consisted of quantifying theoretical inflows to the tunnel through two dimensional numerical simulations of vertical groundwater flow both along the tunnel axis at the tunnel face (axial), and perpendicular to the tunnel (cross-sectional). These calculated inflows were then input as pumping rates to a two dimensional horizontal groundwater flow model. Consequently, this methodology could be considered to represent a combination of the engineering and flow system approaches.

All three models and related simulations were completed using a finite element code. The first two models simulated the vertical flow system through the use of specified head boundaries and treated the tunnel as a head dependent (drain) boundary. The tunnel was

subsequently represented in the horizontal flow model as a specified flux boundary with the calculated flows from the axial simulations representing inflow at the tunnel face and the calculated flows from the cross-sectional simulations representing flows along the tunnel axis behind the face. The advance of the tunnel with time was simulated in the horizontal model by applying the calculated flow for the tunnel face to the leading element for the period of time required to mine the length of tunnel represented by that element (i.e. one time step), followed by application of the calculated flow for areas behind the face (i.e. for subsequent time steps). As such, one time step would be required for each element of the model which the tunnel passes through.

Different groundwater control strategies (advance grouting, installation of 'shotcrete' liner) were also simulated through varying the permeability in a zone around the tunnel during the vertical model simulations. In this way, the authors were able to show that advance grouting ahead of tunnel mining would minimize dewatering effects.

While this latter study is similar in nature to the present study, it differs considerably in the modeling approach implemented (see Section 4.2). In addition, the present study has the advantage of being retrospective in nature and hence a better evaluation of the modeling results and approach used was possible.

1.3 Project Background

The tunneling project, which forms the basis of this study, consisted of the construction of a 2.7-kilometre long subsurface tunnel in Nepean, Ontario, beneath Merivale Road (Figures 1

and 2), between approximately January of 1994 and August of 1995. The 2.25 metre diameter tunnel was constructed for the Regional Municipality of Ottawa-Carleton (the Region) to serve as a portion of a main trunk sanitary sewer, the West Rideau Collector. For most of the sewer alignment, the tunnel was advanced through dolostone bedrock of the Oxford Formation at depths ranging from approximately 15 to 20 metres below the ground surface (excepting the southern portions of the alignment, where the tunnel was completed in overburden materials consisting of marine clay and glacially deposited silt and till). This study focuses on dewatering impacts due to mining of approximately the northernmost 1.4 kilometres of the tunnel (i.e. up to approximately Access Shaft No. 1, as described below).

The tunnel was constructed using a tunnel boring machine (TBM), which advances the tunnel face through a rotary grinding action with carbide cutters. Rock cuttings were passed from the tunnel face by means of a conveyer system to the rear of the TBM and subsequently loaded into 'muck' cars on rails. These were then transported to an access shaft by a small electric locomotive and the cuttings were unloaded at surface through the use of a crane. For mining of the northern portion of the tunnel, the cuttings were removed at the MacFarlane Access Shaft. After the TBM had advanced the tunnel to approximately 1.4 kilometres, the cuttings were removed at Access Shaft No. 1 (see Figure 2).

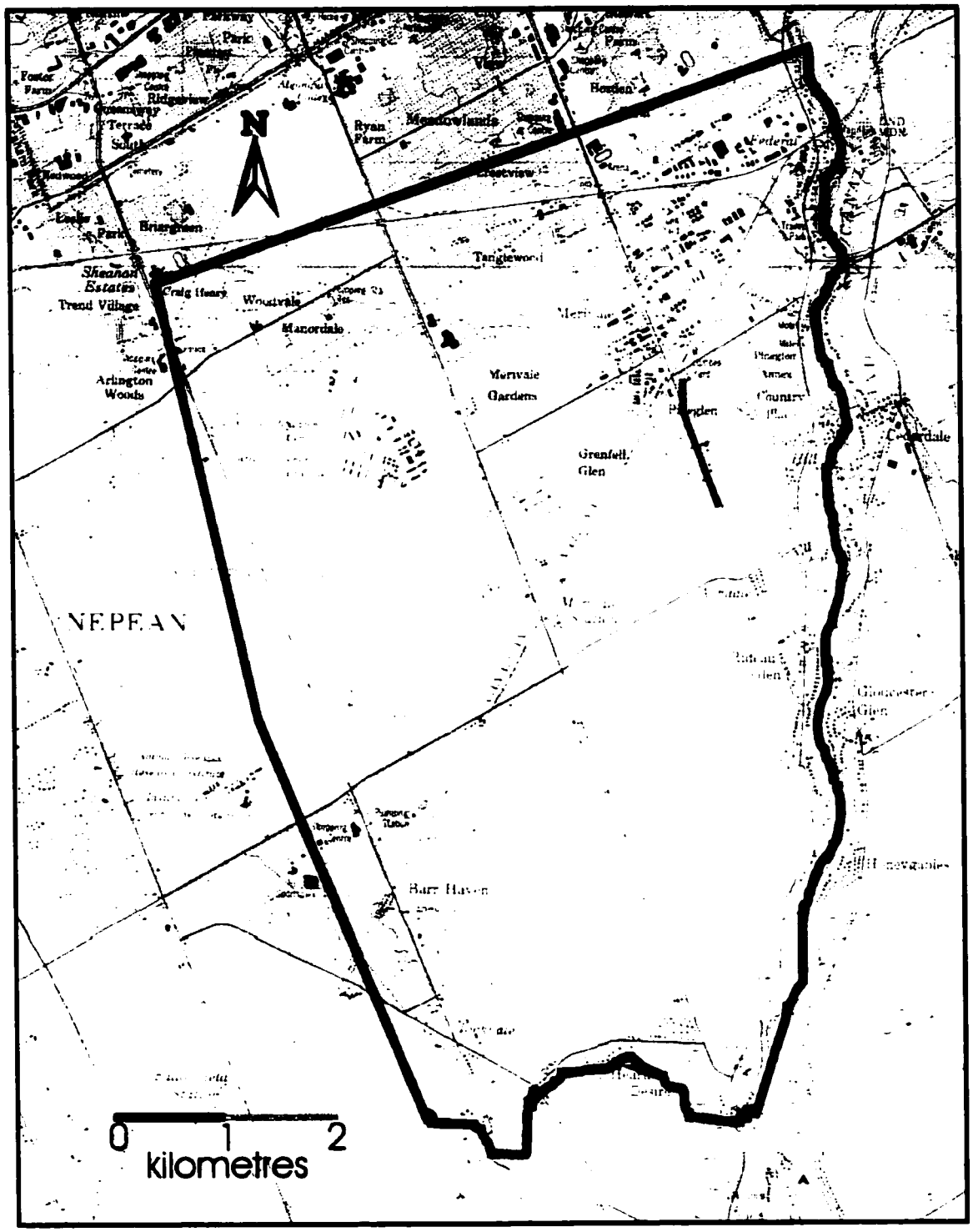

Figure 1 Site Plan – the site (and the model domain) consists of the area bounded by the black line. The blue line shown in the central-eastern portion of the model domain indicates the location and length of tunneling simulated in this study. The site is bounded to the east by the Rideau River, and to the south by the Jock River.

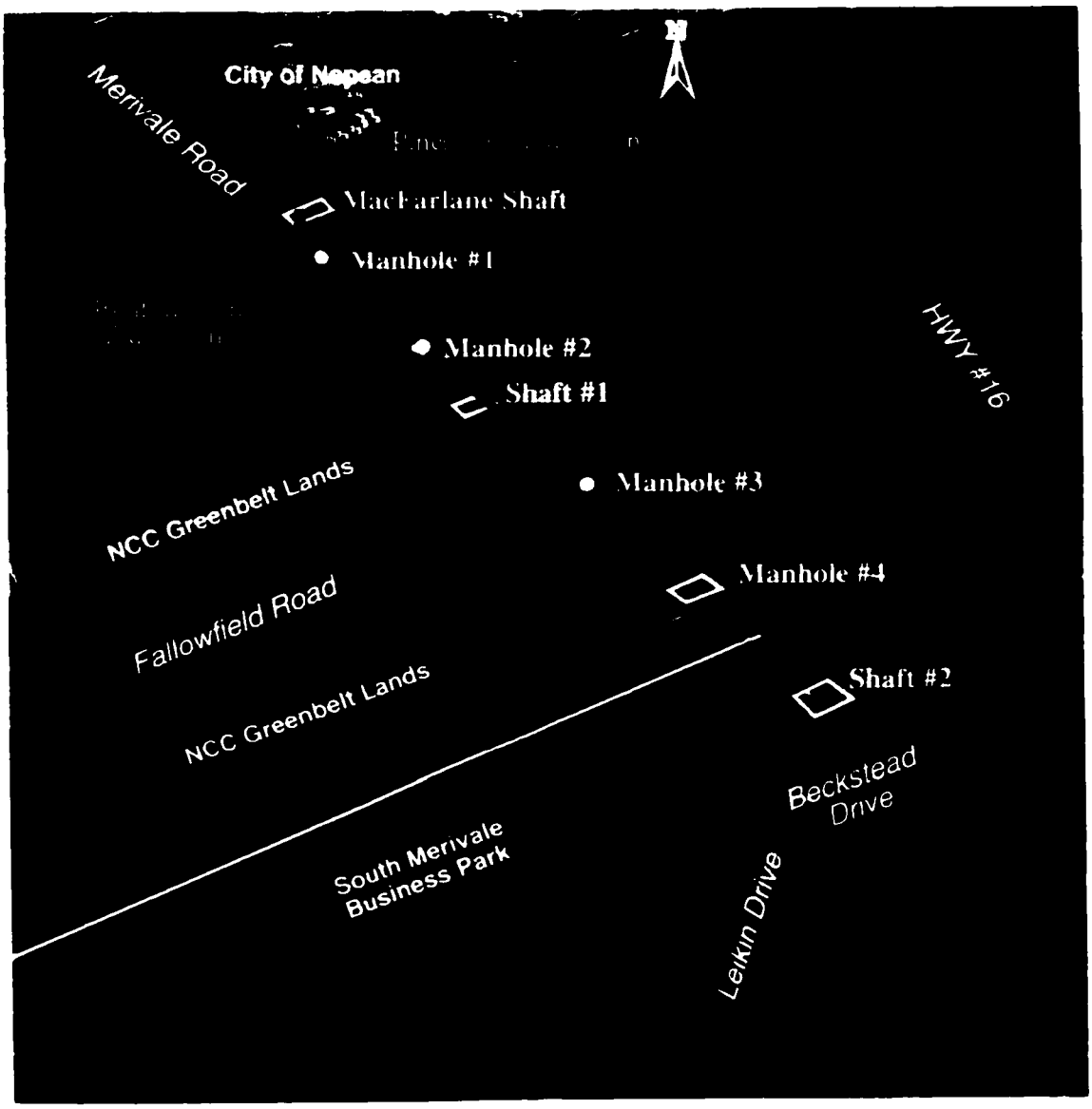

Figure 2 Study area – aerial photograph showing primary area of interest. The locations of significant tunnel structures are shown. This study simulates dewatering impacts as a result of the advance of the tunnel from just south of the MacFarlane Shaft to approximately Shaft #1 to the south, as shown in blue (a distance of 1.4 kilometres).

As stated earlier, the tunnel alignment passed directly through a residential area where homes are serviced through private well water supplies. A design stage hydrogeological study completed by the Region's consultant, Oliver Mangione McCalla and Associates (OMM, 1993a), revealed that the vast majority of the water wells in the vicinity of the northern portion of the proposed tunnel alignment (Pineglen and Grenfell Glen subdivisions - see Figure 2) were either completed and/or obtained water at depths in the same range as the proposed tunnel. OMM also completed pumping tests of two test wells constructed along the tunnel alignment (TW1 and TW2). Analysis of the pumping test data revealed the local aquifer to be highly transmissive.

In order to establish a conservative estimate of the potential magnitude of groundwater inflow to the tunnel, OMM applied the Goodman approach (see Section 1.2.1) using parameter estimates based upon the proposed tunnel configuration and the information available at that time concerning local hydrogeology. The predicted inflows for the modeled range of hydraulic conductivities varied from approximately 6 to 100 litres/minute/metre of tunnel (OMM, 1993a).

The resulting drawdown which might be expected due to groundwater withdrawals at a predicted flow rate of 6 litres/minute/metre of tunnel was calculated by assuming the tunnel to be analogous to a series of pumping wells and applying the analytical solution of Hantush and Jacob (1955). The results of this analysis provided an indication that even at the lowest predicted rate of inflow, hydraulic heads along the tunnel alignment could be lowered to the level of the tunnel. Given the calculated aquifer transmissivity, it was concluded that

widespread well interference problems could occur (OMM, 1993a). This potential was further compounded by the fact that many of the private wells in the vicinity of the tunnel alignment were equipped with shallow lift pumping systems (i.e. able to pump an equivalent head to a maximum of one atmosphere). As such, the available drawdown in these wells would be significantly limited by the pumping system (i.e. the pump would not be able to obtain water from deeper levels in the well, even though plentiful water may be available).

In order to mitigate the potential for well interference problems, the contract between the Region and the tunneling contractor (the Contractor) specified that uncontrolled dewatering would not be permitted and that methods to control the inflow of groundwater should be implemented. The primary means of groundwater control employed by the Contractor consisted of vertically selective pressure grouting of the rock mass through which the tunnel would be constructed (i.e. in advance of tunnel mining activities) in an attempt to locally reduce the hydraulic conductivity of aquifer materials (see Photo 1). This grouting was accomplished by drilling grout holes from the ground surface to a depth of approximately 2 metres below the proposed tunnel invert and selectively grouting the interval to a depth of 2 metres above the tunnel obvert (or crown) through the use of inflatable packers (McKee et al., 1994). Cementitious grout was subsequently pumped from the surface under pressure into this vertical interval.

Groundwater control was also accomplished through the placement of both chemical and cementitious grout from within the tunnel. These grouting activities were concentrated at areas of significant groundwater inflow associated with vertical fractures/fracture zones and

horizontal bedding planes (see Photos 2 and 3). A significant limitation to this method of groundwater control was the fact that these grouting activities could generally not be completed when active mining was underway. Furthermore, grouting activities at the tunnel face required backing up the TBM in order to provide access (see Photo 4). Nevertheless, significant interior grouting activities were completed, particularly during periods when the TBM was shut down for repairs. Groundwater inflow in the northern portion of the tunnel was ultimately reduced to relatively minor levels through more concerted interior grouting operations which were implemented once the TBM had advanced past Access Shaft No. 1 (since grouting could then be completed without interfering with mining operations). Once groundwater inflow was sufficiently controlled, the primary concrete liner for the sewer was poured (see Photo 5), further reducing groundwater inflow to negligible levels.

In order to provide an indication as to the performance of the groundwater control procedures and determine when additional control procedures should be implemented, an elaborate monitoring program was implemented by OMM wherein groundwater levels were measured at monitoring well locations on a regular basis through both manual and electronic recordings (submersible pressure transducers and data loggers). Critical water level elevations were established for each monitoring point wherein any drawdown beyond these levels would be likely to reflect a high probability of interference problems with adjacent domestic wells. Pumping rates from the tunnel were also recorded on a regular basis. This data provides the basis for calibration of transient model simulations undertaken for this study. In addition,

baseline groundwater quality samples were collected at all households within 200 metres of the tunnel alignment prior to the initiation of construction activities.

As tunnel mining proceeded, significant groundwater inflows were recorded. After mining 200 metres, the average pumping rate was approximately 400 litres/minute, or 2 litres/minute/metre of tunnel. By the time the tunnel had advanced 1,400 metres (approximately 6 months), the pumping rates had risen as high as 1,200 litres/minute (0.86 litres/minute/metre of tunnel). Groundwater levels dropped steadily throughout this period and had dropped below the prescribed critical elevations at some monitoring wells within two months of the commencement of tunnel mining activities. Maximum drawdowns at most monitoring wells adjacent to the northern portion of the study area were recorded during mid to late October, 1994. After this time, water levels began to recover due to the interior grouting activities, which occurred once the TBM had passed Access Shaft No. 1. On average, the maximum drawdowns recorded were approximately 3 to 4 metres below the expected seasonal levels and 2 to 3 metres below the prescribed critical levels.

As predicted, numerous well interference problems were experienced due to drawdowns of this magnitude (i.e. heads lower than the prescribed critical levels). Since procedures for dealing with such problems were set out as part of the contract, these were generally resolved in a satisfactory manner. Where the problems involved loss of water quantity, they were usually resolved through the supply of a temporary water supply, upgrading the well's pumping system, or constructing a new well. When a water quality impact was confirmed,

Photo 1 View of grout hole exposed as a result of rock blasting operations (grout hole constructed as part of pre-grouting operations from surface). Note some visible migration of grout in sub-horizontal fracture near top of exposed column of grout (remainder of column not visible due to oblique intersection with exposed rock face).

Photo 2 View of large vertical fracture zone or fault intersecting approximately perpendicular to tunnel heading. Note plastic tubing emerging from fracture zone used for channeling water to facilitate grouting operations.

Photo 3 View of vertical fracture sealed with chemical grout.

Photo 4 Discharge of groundwater from a bedding plane at the tunnel face. Object at right is one of the cutting heads of the tunnel boring machine (which has been backed away from the face).

bottled water was supplied as a temporary measure. In some instances, chronic water quality problems were dealt with through the installation of water treatment equipment.

The most common water quality problem experienced involved the migration of highly mineralized water (which existed prior to construction) from one area in the Pineglen subdivision towards the tunnel due to the altered groundwater flow patterns resulting from construction dewatering. As such, numerous households which had previously been supplied with relatively fresher water experienced significant increases in parameters such as hardness, sulphate and chloride. By and large, water quality at the affected households recovered to pre-construction conditions after groundwater flow patterns returned to normal.

Well interference problems were confirmed at approximately 34 households in the Pineglen and Grenfell Glen subdivisions. Of these, 20 involved water quantity problems alone, 8 involved water quality problems alone, and 6 involved both water quantity and quality problems. In addition to these confirmed problems, numerous complaints were responded to, which were determined to be unrelated to tunnel mining activities. The potential for well interference in these areas was ultimately eliminated through the placement of the concrete liner within the tunnel.

Photo 5 Workers placing forms for pour of concrete liner. Note section shows 3 bedding layers with middle layer being significantly less competent than both the overlying and underlying layers. A vertical fracture approximately perpendicular to the tunnel heading can be seen in the foreground.

As stated previously, one of the objectives of this study was the use of a calibrated model for the running of predictive simulations of alternate construction scenarios. These are presented in Section 6.0 and include simulations of the effect of faster mining rates, more intensive grouting, no grouting, and grouting combined with artificial aquifer recharge through the use of injection wells.

1.4 Modeling Approach

Following from the objectives outlined earlier and given the wealth of retrospective data available (as described above), it was clear that this study required the use of numerical groundwater flow modeling techniques. The modeling protocol used generally followed the steps outlined below, as suggested by Anderson and Woessner (1992).

1) Define purpose	- satisfy objectives as outlined above;
2) Develop Conceptual Model	- assemble field data; - define hydrostratigraphic units and system boundaries;
3) Select Code	- description and justification of codes used (MODFLOW, MT3D);
4) Model Design	- translate conceptual model into form suitable for computer modeling;
5) Model Calibration	- assignment of realistic parameter values which allow the model to reproduce field measured heads (steady state and transient); - sensitivity analysis;

6) Model Verification - use of calibrated model to reproduce other field measured heads and flows (transient);

7) Prediction - quantification of the response of the system to hypothetical construction scenarios;

8) Presentation of Results - presentation of model design and results (the following sections of the thesis).

Acknowledgments

The author would like to take this opportunity to express his appreciation to those people who provided support and guidance during this project. Notably, Dr. Michel Robin, as supervisor, provided helpful suggestions and guidance throughout the completion of this thesis.

Gratitude is owed to both the author's employer, Oliver Mangione McCalla and Associates (OMM), and the Regional Municipality of Ottawa-Carleton for allowing the use of the data originally collected for the purpose of the tunnel construction project.

Mr. John McKee of OMM provided the original encouragement to pursue this project and had valuable input in the form of technical review. Other colleagues at OMM who deserve thanks include Mr. Stephen Wilson for technical review and assistance, Mr. Robin Gardner for assistance with some of the graphics included within this thesis, and Mr. Michel Kearney, for translation of the abstract.

My deepest appreciation is however reserved for my wife Sheila (SP), who in addition to helping tabulate the water well record data and acting as 'rodman' during the collection of some elevation data, provided abundant encouragement and support, without which the completion of this project would not have been possible.

2.0 Conceptual Model

This section presents the physical and hydrogeologic setting of the area modeled and describes the conceptual model upon which the numerical model is based. Please note that the term 'site' is utilized herein to refer to the geographic area which roughly coincides with the model domain (as shown on Figure 1), and the term 'study area' is utilized to represent more specifically the area in the vicinity of the tunnel (as shown in Figure 2).

2.1 Geologic and Physical Setting

2.1.1 Surface Features

The ground surface across the site is generally flat lying, sloping gently from higher lands to the south-west. Elevations range for the most part between approximately 90 and 100 metres above sea level (m.a.s.l.), excepting areas proximal to surface water features.

The largest surface water feature in the area consists of the Rideau River, which flows from south to north and forms the eastern boundary of the site (see Figure 1). A tributary, the Jock River, flows from west to east and forms the southern boundary of the site where it joins the Rideau. Smaller tributaries of the Rideau which also flow from west to east across portions of the site include Nepean Creek (near the northern boundary of the site), Black Rapids Creek (central portion of the site), and the East Barrhaven Creek (south-central portion of the site).

Surface water elevations on the Rideau River range from approximately 78 m.a.s.l. at the southern end of the site to 75 m.a.s.l. at the northern end of the site. Consequently, all of the tributaries flow to the Rideau through significant ravines. The depth of the river is in the

range of approximately 8 to 9 metres within the study area (Canadian Hydrographic Service, 1984).

Based upon the available water level data from monitoring wells constructed for the tunnel project and upon static water levels recorded on Ontario Ministry of the Environment (MOE) Water Well Records, the Rideau River, the Jock River and Black Rapids Creek strongly influence groundwater flow at the site.

Most of the site is artificially drained through ditches, agricultural drains, or storm sewers.

2.1.2 Geology

Surficial deposits exposed within the study area consist of Quaternary aged deltaic or estuarine sands, marine clays and silts, and sand till (Richard, 1976). The sands are described as medium to fine grained and interpreted to have been deposited during the regression of the post-glacial Champlain Sea. These sands represent the youngest strata within the study area and occur over nearly all of the lands to the north of Black Rapids Creek. They are underlain by silts, clays, and silty clays which have been interpreted as offshore marine deposits of the Champlain Sea. These silt and clay deposits represent the surficial deposits over most of the remainder of the study area, excepting further south, near the Jock River, where the sand till is exposed. This unit underlies the clays and silts and is described as a sandy to silty compact glacial till. These overburden materials are deposited unconformably over dolomitic limestone of the Ordovician aged Oxford Formation (Bélanger, et al., 1977).

The overburden deposits have a combined thickness generally ranging between approximately 6 and 19 metres within the study area, as determined from geotechnical and hydrogeological boreholes constructed in the vicinity of the tunnel alignment. The overburden thickness is considerably less within the ravine at Black Rapids Creek, where the bedrock surface is within one metre of the base of the creek at the intersection with the tunnel alignment. Data from the boreholes constructed within the study area prior to tunneling was used to construct a geologic cross-section along the tunnel alignment (OMM, 1993a). A portion of this cross-section is reproduced herein (Figure 3). As depicted on the cross-section, the portion of the tunnel simulated in this study was constructed through the Oxford Formation dolomitic limestone.

The above noted borehole drilling program confirmed the stratigraphic sequence and types of deposits outlined above. Of note, significant lenses of silty sand were encountered at a number of locations either at the base of, or within, the marine silts (see Figure 3). The presence of such deposits, combined with localized thinning of the silt and clay sequences, indicates that the clays and silts could be vertically discontinuous at some locations within the site.

Figure 3 (following page) – Inferred geologic section along northern portion of tunnel alignment. The area shown includes the entire length of tunnel simulated in this study, a total length of 1,400 metres, from approximate chainage 0+100 to 1+500 metres (the northernmost 100 metres was mined earlier in 1994 until a major breakdown of the TBM occurred – since this portion of the tunnel was subsequently well sealed through interior grouting operations prior to restarting mining operations, it was not simulated in this study).

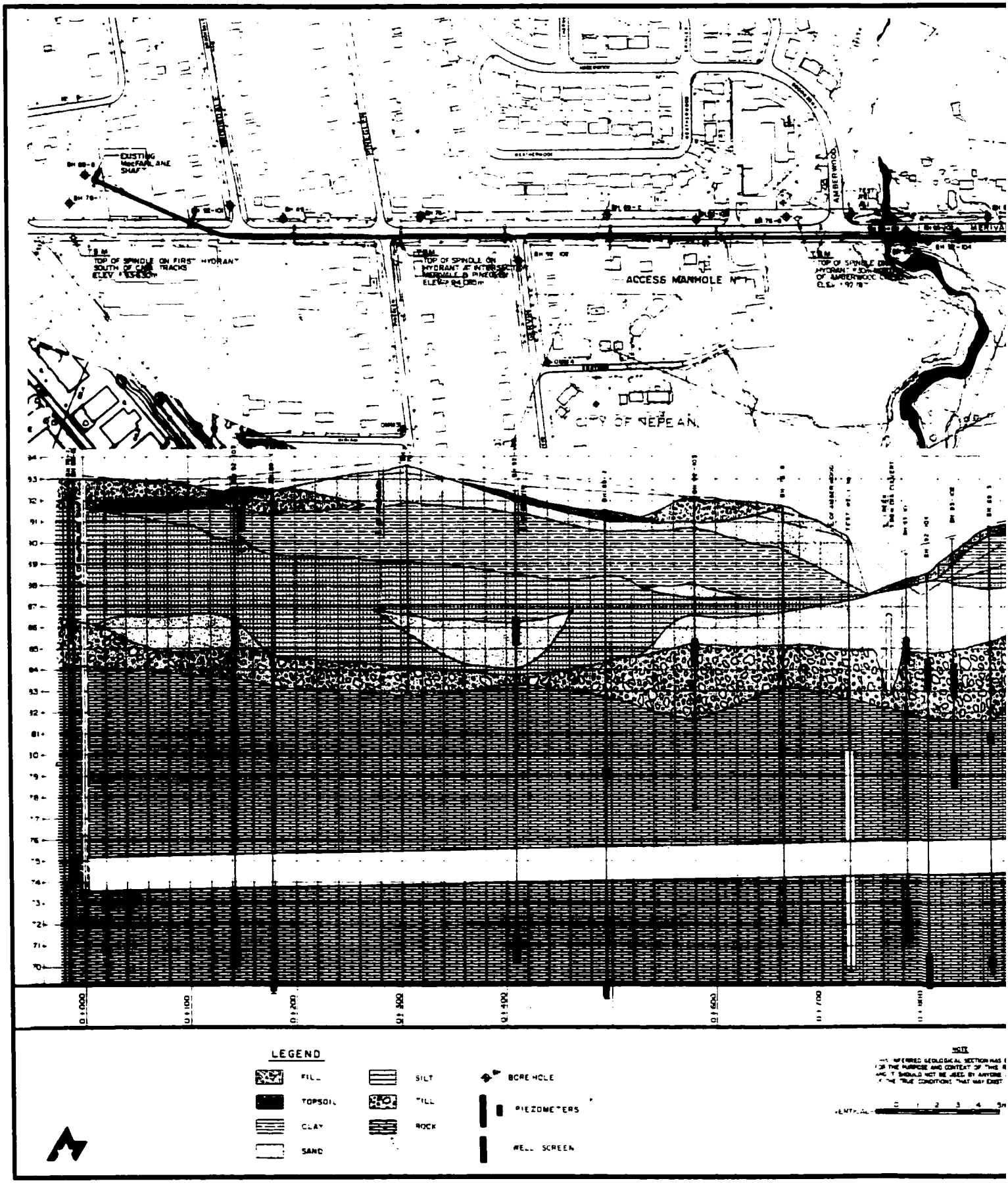
EXISTING MacFARLANE SHAFT
TBM TOP OF SPINDLE ON FIRE HYDRANT SOUTH OF CNR TRACKS ELEV. 93.60m
TBM TOP OF SPINDLE ON HYDRANT AT INTERSECTION OF MERIVALE & PINECREST ELEV. 94.08m
ACCESS MANHOLE
CITY OF NEPEAN
LEGEND
FILL
TOPSOIL
CLAY
SAND
SILT
TILL
ROCK
BORE HOLE
PIEZOMETERS
WELL SCREEN

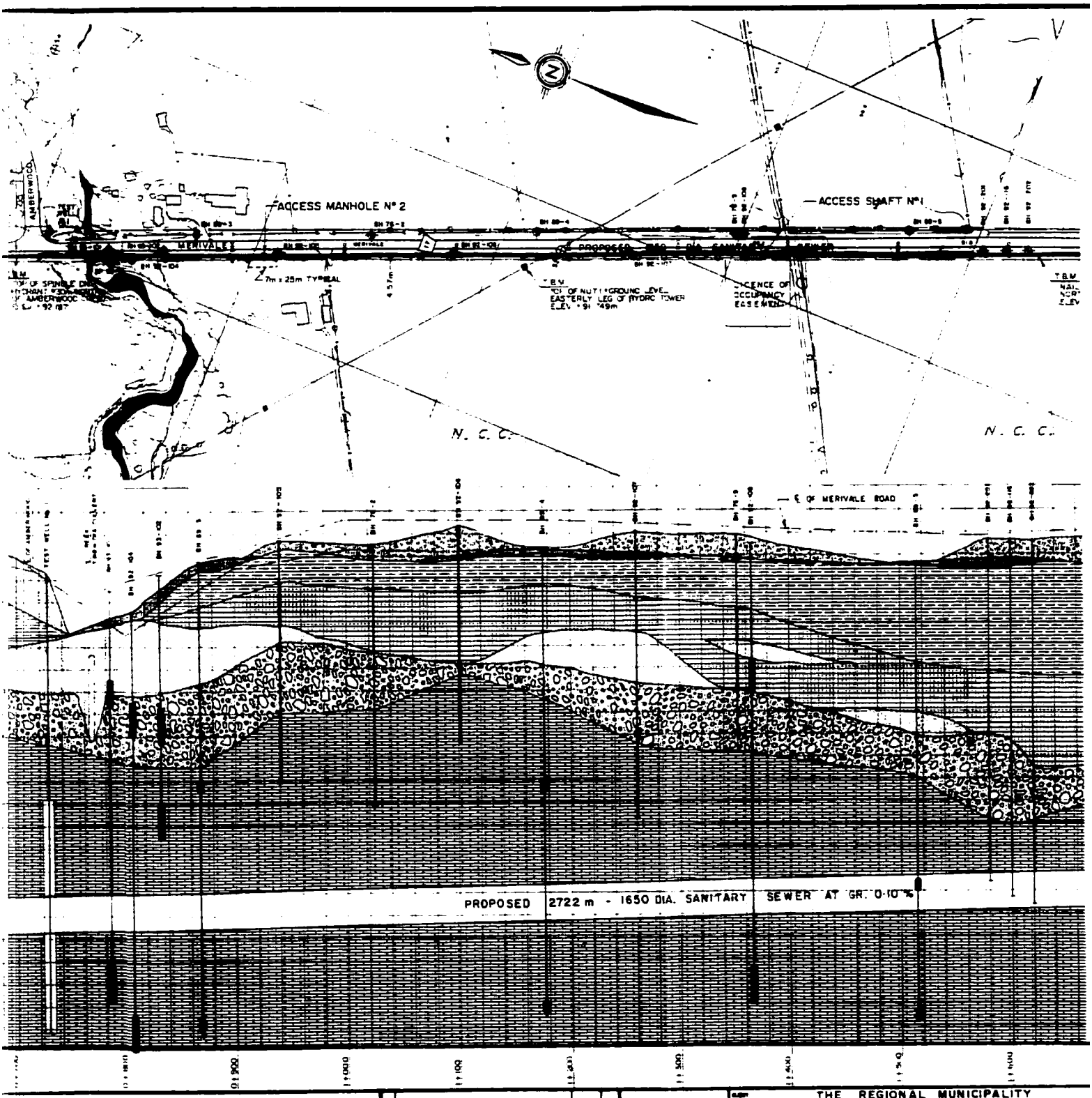

NOTE

THIS INFERRED GEOLOGICAL SECTION HAS BEEN PREPARED FOR THE PURPOSE AND CONTEXT OF THIS REPORT ONLY AND IT SHOULD NOT BE USED BY ANYONE AS AN INDICATION OF THE TRUE CONDITIONS THAT MAY EXIST

VERTICAL 0 1 2 3 4 5m

NO.	REVISIONS	DATE	BY
2	ADDED BH LOGS 93-101, 102, 103	9/3/93	BPL
1	ADDED TW 2 LOG		
	ISSUED FOR CONTRACTOR PRE-QUALIFICATION	5/2/93	BPL

CLIENT: THE REGIONAL MUNICIPALITY OF OTTAWA-CARLETON

PROJECT: WEST RIDEAU COLLECTOR SEWER PHASE III

TITLE: INFERRED GEOLOGICAL SECTION

OLIVER MANGIONE McCALLA & ASSOCIATES LIMITED

DATE: AUGUST 1992 | SCALE: AS SHOWN | DRAWING NO.: FIGURE 3 | SHEET NO.: 2

The borehole drilling program also indicated that the basal till unit contained gravel and boulders at some locations and the upper portions of the bedrock were generally found to be moderately to highly fractured.

Information obtained from MOE Water Well Records confirms the presence of limestone (interpreted as the Oxford Formation) underlying the overburden materials. While the vast majority of the water wells in the area were completed within the Oxford Formation, a few wells are reported as being completed in an underlying sandstone, which is interpreted as either March Formation (Ordovician aged transitional shales and sandstone), or Nepean Formation (Cambro-Ordovician sandstone). Based upon this information, the average thickness of the Oxford Formation within the study area is inferred to be approximately 40 metres.

2.2 Definition of Hydrostratigraphic Units

For the purpose of developing the site conceptual model, the geologic materials outlined above were assessed in terms of their hydrogeologic properties in order to define hydrostratigraphic units. As stated by Anderson and Woessner (1992), hydrostratigraphic units comprise geologic units having similar hydrogeologic properties.

The main water bearing unit in the area (from a water supply perspective) is the dolomitic limestone of the Oxford Formation. From both a physical and a hydrogeologic perspective, this unit is contiguous with the overlying tills and sands (where sand lenses occur in contact with the till). Consequently, these combined sequences are considered to represent one

hydrostratigraphic unit. Specific evidence supporting this interpretation includes the following:

- there is no evidence of any intervening zones of lower permeability,
- the fractured nature of the bedrock interface zone provides a good physical connection between the bedrock and overlying till,
- water level data from multi-level monitoring wells completed within the till showed very similar responses (in some cases nearly identical) to wells completed in the bedrock both under stressed conditions (i.e. due to tunnel dewatering) and seasonal change. In most cases there was a downward vertical gradient (approximately 0.04 m/m), except in the vicinity of Black Rapids Creek, where a gradient reversal was normally observed (i.e. groundwater discharging to creek). Of note, a downward gradient of similar magnitude was observed at locations where multi-level monitors were completed within the bedrock only,
- the results of preliminary model simulations showed that considering the till as a separate unit from the bedrock gave incorrect results under stressed conditions (see Section 3.3).

The clay and silt sequences that overlie the till are considered to represent a confining aquitard with respect to the till/bedrock unit, and consequently are defined as a separate hydrostratigraphic unit. The silt sequence is included with this unit since borehole descriptions describe it as having a significant clay component and since it is considered to have been deposited in a similar depositional environment to the clay sequence. Water level

data for this unit was generally not collected within the study area. However, data collected from monitoring wells located south of the study area during subsequent mining activities (for a later extension to the sewer) confirmed that the response to construction dewatering was significantly different (slower to respond and lower in magnitude) in the clay than in the till/bedrock unit.

The uppermost sequence within the study area, consisting of the deltaic or estuarine sands, as well as any surficial topsoil and fill, are considered to be of little significance in terms of the local groundwater flow regime since these materials would likely only be seasonally saturated based upon their limited thickness and the presence of artificial surface drainage features throughout the site.

2.3 Hydrogeology

The most significant hydrostratigraphic unit in terms of water supply and tunnel construction considerations is the till/bedrock unit since it represents the water source for the vast majority of the domestic wells in the area and since the tunnel was constructed through this unit. Information pertaining to the hydrogeological characteristics of this unit was available from the design stage studies for the tunnel project (OMM, 1993a) and sources such as MOE Water Well Records.

2.3.1 Hydraulic Heads

As indicated previously, a vast amount of data relating to hydraulic head distributions in the till/bedrock unit was collected during the course of the tunnel project (both stressed and

steady state). This information was collected primarily from monitoring wells constructed specifically for the purposes of the project and consequently the data points are concentrated along the tunnel axis. Data representing steady state head conditions was collected for this study on June 6, 1996 at all available monitoring well locations within or in proximity to the study area and supplemented by data from a small number of private water wells that were amenable to water level measurements. A plot depicting steady-state equipotential lines within the study area is presented as Figure 4.

As shown on Figure 4, the groundwater flow direction in the study area is generally eastwards, towards the Rideau River. However, Black Rapids Creek acts as a significant local influence on groundwater levels and clearly acts as a point of groundwater discharge under steady-state conditions (i.e. is gaining). This is confirmed by the fact that multi-level monitoring wells in proximity to the creek indicated an upward gradient in this area. Of note, this gradient was reversed during periods of maximum drawdown associated with tunnel dewatering, although no significant impact in terms of creek water levels was observed.

The contour plot also shows a small number of anomalous data points, indicative of some mounding of water levels at a couple of locations (specifically at the 88.0 metre potentiometric contour). All data points were included for the purposes of model calibration despite this. It is likely that this effect reflects the fact that the data is derived from wells screened at different depths in the presence of a vertical gradient.

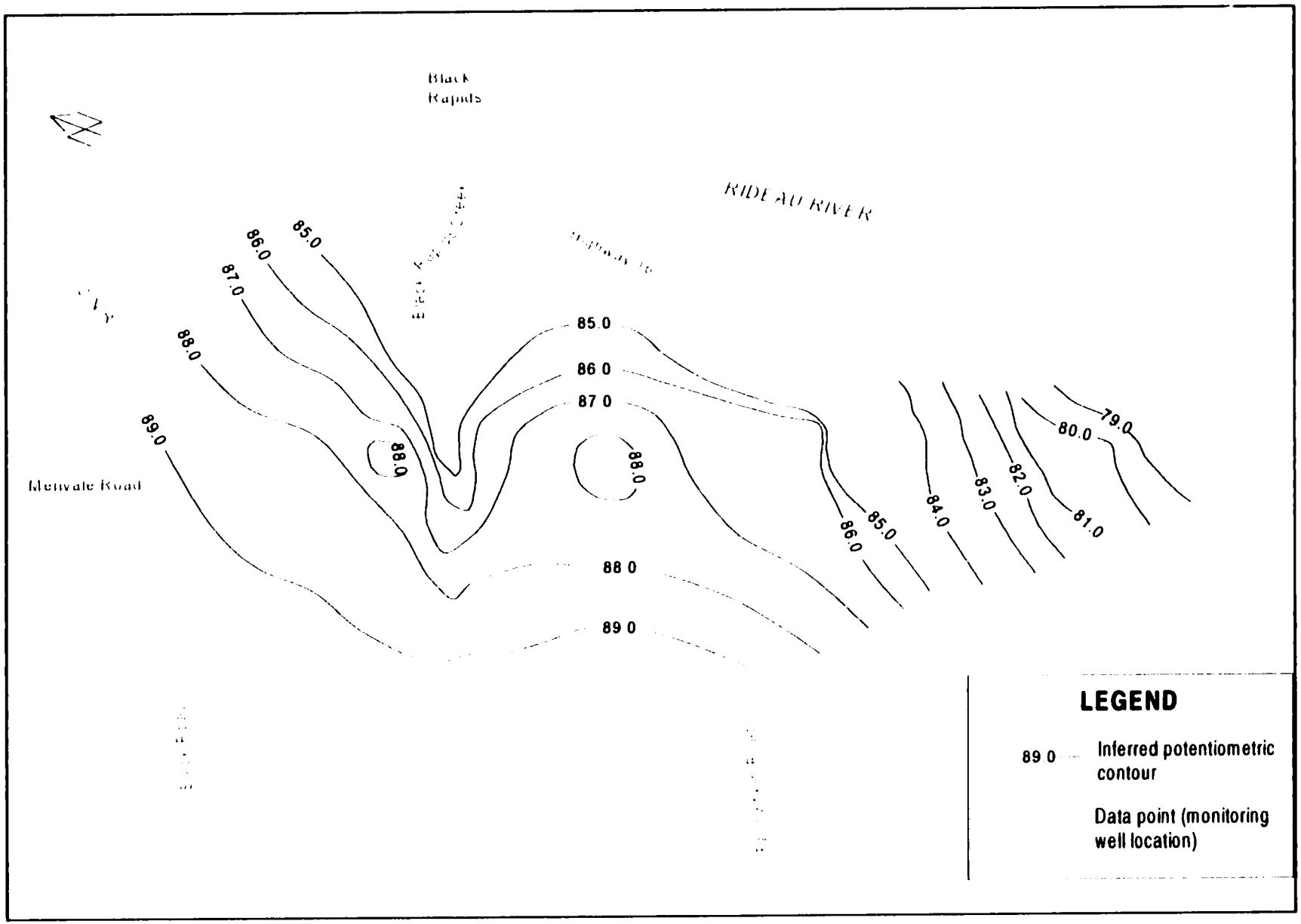

Figure 4 - Contour Plot of Observed Heads in the till/bedrock hydrostratigraphic unit (June 6, 1996)

2.3.2 Aquifer Top Elevation

For the purpose of this study, top elevations for the till/bedrock unit were collated from borehole logs associated with the tunnel project and from MOE Water Well Records. In areas where abundant wells were located (e.g. within residential subdivisions), data was selected from a representative number of locations (average density of approximately one well per 300 square metres)[1]. Where data points were more sparse, all available information was reviewed. The resulting database consisted of 68 data points (this data is presented in Appendix A as Table A2). A contour plot (Figure 5) of aquifer top elevations across the site was generated from this data through kriging with a linear variogram model using a commercial contouring software package (Surfer Win32 by Golden Software). As depicted in Figure 5, the aquifer top elevations across the site varied between approximately 67 and 86 m.a.s.l.

Based upon the inferred aquifer top elevations at the Rideau River, and the known depth of the river in this area, the Rideau River partially penetrates the till/bedrock unit along most of its length across the site. With respect to the Jock River, the available elevation data was insufficient to conclusively determine whether such a relationship also exists along its length. However, water level evidence from MOE Water Well Records adjacent to the Jock River suggested that the till/bedrock unit is hydraulically connected to the river.

---

[1] In the case of MOE Water Well Records, an attempt was made to collect data from records that provided more complete lithological descriptions.

2.3.3 Transmissivity and Storativity

Aquifer transmissivity was calculated by OMM (1993a) from data collected during two pumping tests conducted as part of a design stage study for the tunnel project. The pumping tests were completed at two different pumping well locations, test well 1 (TW1) and test well 2 (TW2). TW1 consisted of a bedrock well just north of Black Rapids Creek (approximately 725 metres along the tunnel alignment) and TW2 consisted of an overburden well screened within the till approximately 400 metres south of Fallowfield Road (approximately 2,400 metres along the tunnel alignment). Distance/drawdown data collected during these pumping tests at numerous monitoring wells was evaluated analytically by OMM.

The calculated transmissivity values from the TW1 pumping test ranged over less than one order of magnitude. The mean (arithmetic) transmissivity reported by OMM was 1.3×10^{-3} m^2/sec. Similarly, transmissivity values from the TW2 pumping test were also consistent, varying just over 1 order of magnitude and having an arithmetic mean of 9.5×10^{-4} m^2/sec. Using assumed average thicknesses of the aquifer gave an average hydraulic conductivity of 2.2 m/day. Details are presented in Section 3.6.1.

Storativity values calculated from both pumping tests were also fairly consistent, with all of the values ranging just over one order of magnitude for the TW1 pumping test, and most of the values from the TW2 pumping test varying by less than one order of magnitude. The arithmetic means of the storativity values were 1.1×10^{-3} for the TW1 test, and 8.9×10^{-4} for the TW2 test. Calculated transmissivity and storativity values are presented in Appendix A (Table A1).

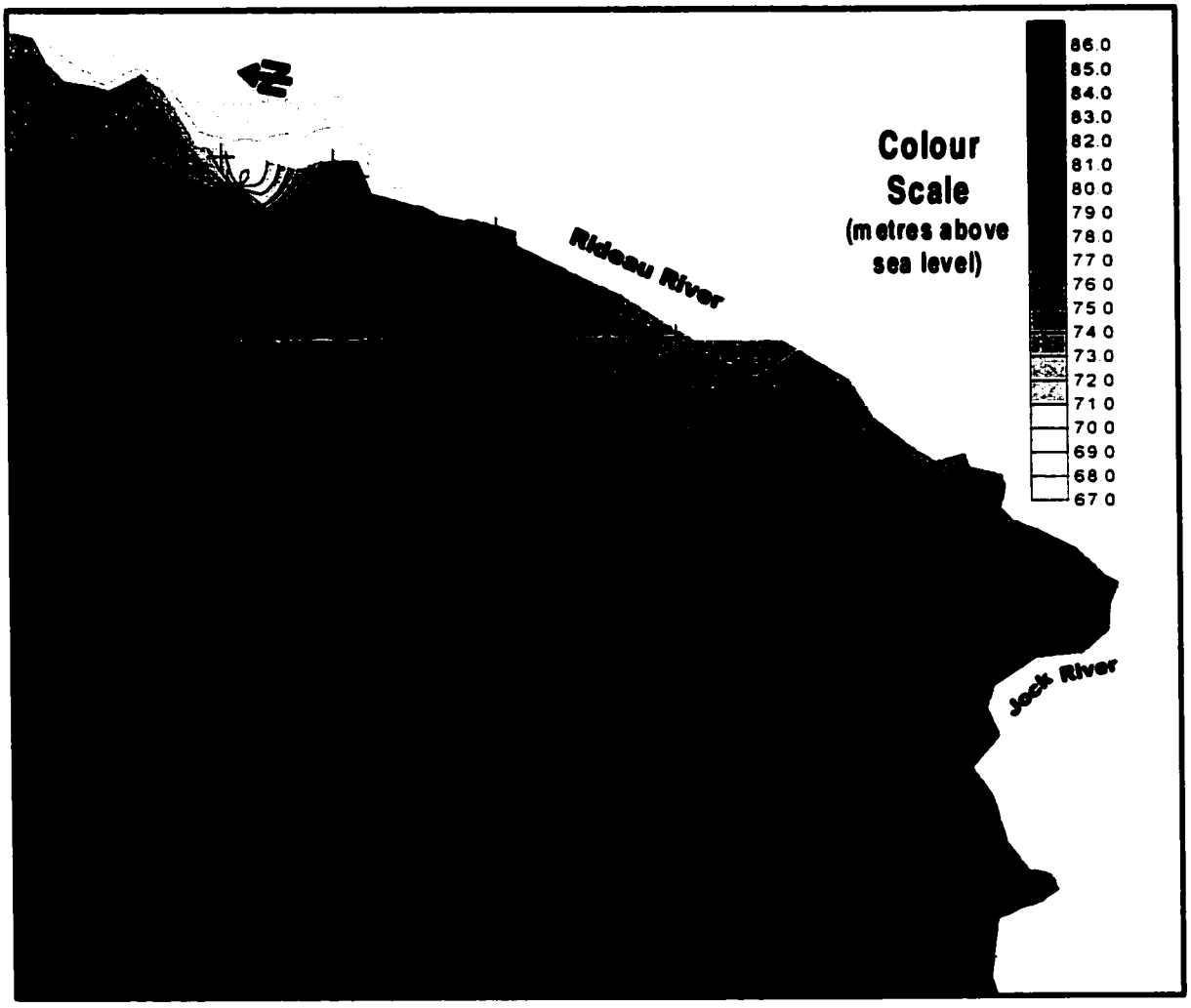

Figure 5 Aquifer top elevations – contour plot of inferred top elevation of till sequence. Data points are indicated by '+' symbols.

3.0 Model Design

Based upon the conceptual model outlined above, a numerical model was designed. The model code, input parameter values, and relationship to the conceptual model are described hereafter.

3.1 Model Code

In terms of groundwater flow modeling, the model code chosen for this study consisted of MODFLOW, a three-dimensional finite difference code developed by the United States Geological Survey (McDonald and Harbough, 1988).[2] MODFLOW is the most widely used and accepted code in the industry. It was considered to be particularly suitable for this application due to its ability to handle a wide range of boundary conditions (including head-dependent boundaries such as drains and rivers), and its ability to simulate transient stresses. In addition, a number of contaminant transport codes have been developed for use with the output from block-centred finite difference flow models such as MODFLOW. Amongst these is MT3D (Zheng, 1990), which simulates advection, dispersion and chemical reactions of dissolved chemicals in groundwater systems using a mixed Eulerian-Lagrangian approach. As such, MT3D was used to simulate the migration of a zone of highly mineralized groundwater in response to tunnel dewatering.

[2] The PCG2 solver package (Hill, 1995) was used with MODFLOW, using modified incomplete Cholesky preconditioning.

The main potential limitation associated with the use of MODFLOW for this application involves the simulation of groundwater flow in fractured bedrock. Since MODFLOW is intended for simulation of flow in porous media having continuous interconnected pore space, its use for simulations of flow in fractured bedrock implies that the rock is being represented as an equivalent porous medium (EPM).

The EPM approach assumes that the primary and secondary porosity and the hydraulic conductivity of the fractured rock can be represented by a continuous porous medium having so called "equivalent" or "effective" hydraulic properties (Anderson and Woessner, 1992). This assumption requires that these effective hydraulic properties are valid for a given volume of fractured rock (termed the "representative elementary volume", or REV). Consequently, the approach may have limited applicability in many situations at smaller or local scales. For example, the approach would likely not be valid when both the fracture porosity and the unfractured block hydraulic conductivity are low, even with a large REV (Gale, 1982). Despite this, most researchers appear to agree that in most cases an EPM approach will adequately represent the behaviour of a regional flow system. However, there is disagreement on the applicability of the approach at a smaller scale (Anderson and Woessner, 1992).

In spite of these potential limitations, the use of an EPM approach was considered appropriate for this study for several reasons:

1. Visual observations within the tunnel revealed that groundwater flow within the bedrock is predominantly through vertical fractures and horizontal bedding planes. Furthermore, the density of these features was observed to be sufficient to provide a continuous interconnected flow regime on the scale of metres to tens of metres (based on qualitative judgement).

2. The aquifer (the hydrostratigraphic unit defined by the till/bedrock) includes porous media (silty to sandy till and sand).

3. Application of a discrete fracture or dual porosity model would be more difficult given the available data and the objectives of this study, and may be less appropriate given the considerations outlined above.

3.2 Model Domain

The model domain consisted of a grid of 108 rows and 130 columns (14,040 cells) covering an area of 70.3 square kilometres. 10,422 cells were active, representing an area of approximately 40 square kilometres, while the remainder of the model was inactive (no flow cells). The active area of the model domain is delineated on Figure 1. The full model domain is depicted on Figure 6a.

The grid spacing ranged from as small as approximately 2.5 metres along the tunnel axis to 100 metres at locations more distant from the study area. This refinement in grid spacing in the vicinity of the tunnel was necessary in order to realistically represent the physical dimensions of the tunnel itself and to provide a more accurate simulation of the hydraulic

gradient in the vicinity of the tunnel (under stressed conditions). Consequently, it was necessary to orient the model domain parallel to the tunnel axis. This restriction accounts for the relatively large portion of the model domain which is inactive.

3.3 Number of Layers

The model consisted of a single layer representing the till/bedrock unit described in Section 2.2. The layer type was specified as confined. As such, the transmissivity and storativity of the layer were held constant throughout the simulations.

Preliminary modeling efforts consisted of a two layer model wherein the till and bedrock were treated as separate layers in order to simulate the observed vertical gradient within this combined unit. The results of these modeling efforts showed that the overall flow field, including the observed vertical gradient, could be well simulated under steady state conditions through contrasting the vertical hydraulic conductivity between the two sequences. However, the simulated flow field deviated significantly from that actually observed when stressed conditions were simulated (little or no response within the till). This led to the conclusion that treating these sequences as separate layers was inappropriate.

While the vertical gradient through the till/bedrock unit could still be simulated through leakage to an underlying layer, the introduction of such a layer was deemed unnecessary since: i) the vertical flow component under stressed conditions (i.e. due to tunnel dewatering) would not be significant, ii) since the hydrogeologic characteristics of the deeper bedrock

have not been evaluated within the area, and iii) since the addition of such a layer would unnecessarily increase the complexity of the model.

3.4 Boundary Conditions

Boundary conditions were selected based upon the requirement to simulate the conceptual model outlined previously and upon the results of preliminary modeling efforts.

3.4.1 Specified Head Boundaries

A part of the western boundary of the active portion of the model consists of constant head cells. The head at these nodes was specified as 90 m.a.s.l., which was considered to be a realistic value for the vertically averaged head in the till/bedrock unit at this location. This constant head boundary served two purposes: i) firstly, it provided a source or sink of water flowing into or out of the model domain from the western boundary of the study area, and ii) it satisfied the requirement that head be specified as constant for at least one node in order to give the model a reference from which to calculate heads (Anderson and Woessner, 1992). Based upon topography and surface water drainage patterns, the location of this constant head boundary likely approximates the general area of a groundwater divide between water flowing eastwards and discharging to the Rideau River, and water flowing northwards, towards the Ottawa River.

It was recognized that constant head conditions are not physically representative of this location since they provide an infinite source or sink of water. However, the use of this type of boundary will not impair the modeled flow system within the area of interest, so long as

the boundary is located sufficiently distant from the location of any transient stresses (e.g. the tunnel, in this case). This type of boundary condition usage is considered to be an accepted practice in groundwater flow modeling applications (Anderson and Woessner, 1992). For this model, the size of the model domain was established through preliminary modeling efforts (i.e. boundary effects were observed during transient simulations with a smaller domain).

3.4.2 Specified Flow Boundaries

North and West Boundaries

The north model boundary and a portion of the west model boundary consisted of no-flow boundaries located at distances which were determined to be sufficiently remote from the study area to minimize any boundary effects during transient (stressed) simulations (based upon preliminary modeling).

Top and Bottom Boundaries

The upper boundary of the model is defined by the upper surface of the till/bedrock unit and was represented as a specified flux boundary using MODFLOW's recharge package. In this way, recharge to the aquifer via downward flux from the overlying silts and clays was represented. It was recognized that this boundary would not simulate a leaky response under stressed conditions (due to possible leakage from the overlying silt/clay)[3]. However, allowing for such leakage in the model was not considered necessary since it would likely not

[3] OMM (1993a) reported that evidence of leakage in drawdown response was observed in some monitoring wells during the TW1 pumping test.

have a large effect on the overall response of the aquifer. Furthermore, sufficient data was not available to support the simulation of this overlying layer (which would also result in an unjustified increase in the complexity, and associated uncertainty, of the model).

The lower boundary of the model was represented as a specified flux (no-flow) boundary (at a uniform elevation of 36 m.a.s.l.).

Source Area of Highly Mineralized Water

As outlined previously, pre-construction baseline water quality analysis at households in the vicinity of the tunnel alignment identified a zone of relatively more highly mineralized groundwater to the east of the northernmost end of the tunnel, which is assumed to be naturally occurring. Further water quality analysis completed as tunnel dewatering was underway revealed that more mineralized water from this source area had migrated towards the tunnel in response to pumping, resulting in the deterioration of water quality at a number of households. The source area of this more mineralized water (see Figure 6b) was therefore represented as a zone of constant concentration (which is numerically equivalent to a specified flow boundary), using chloride as an indicator parameter (at a concentration of 400 mg/L). In this way, the migration of dissolved chloride could be simulated during transient modeling with the use of MT3D. Of note, chloride concentrations within the source area were observed to remain relatively consistent throughout monitoring activities completed before, during and after the period of construction, indicating that the use of a constant concentration boundary is conceptually appropriate.

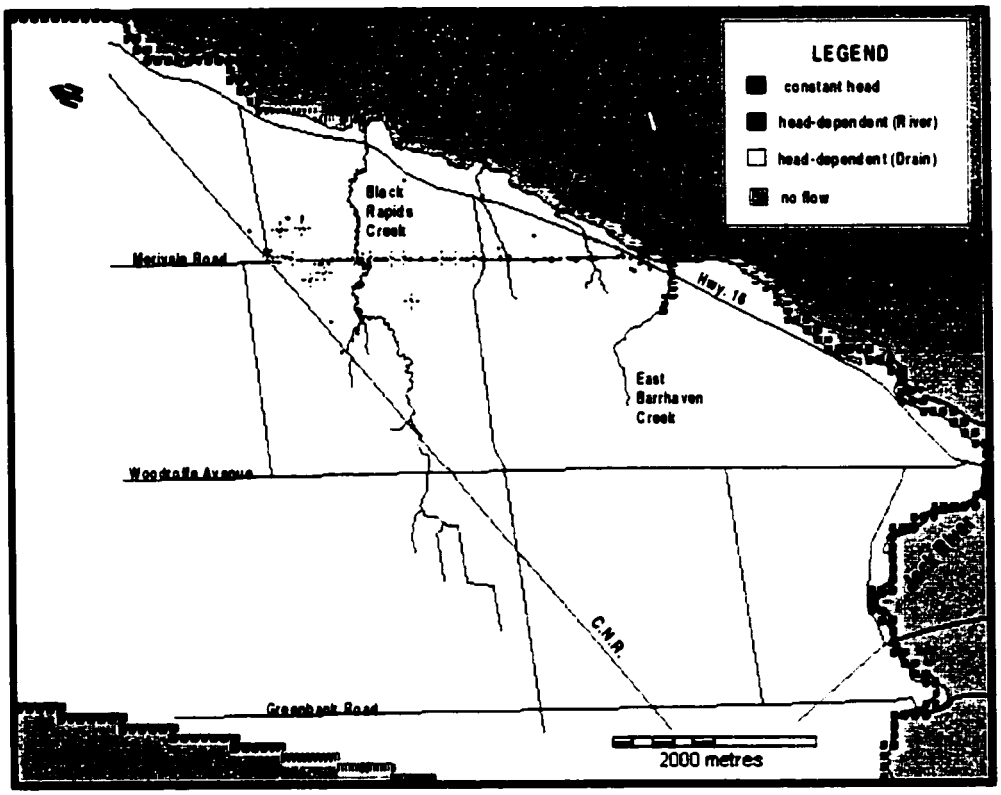

Figure 6A Model domain and boundary conditions

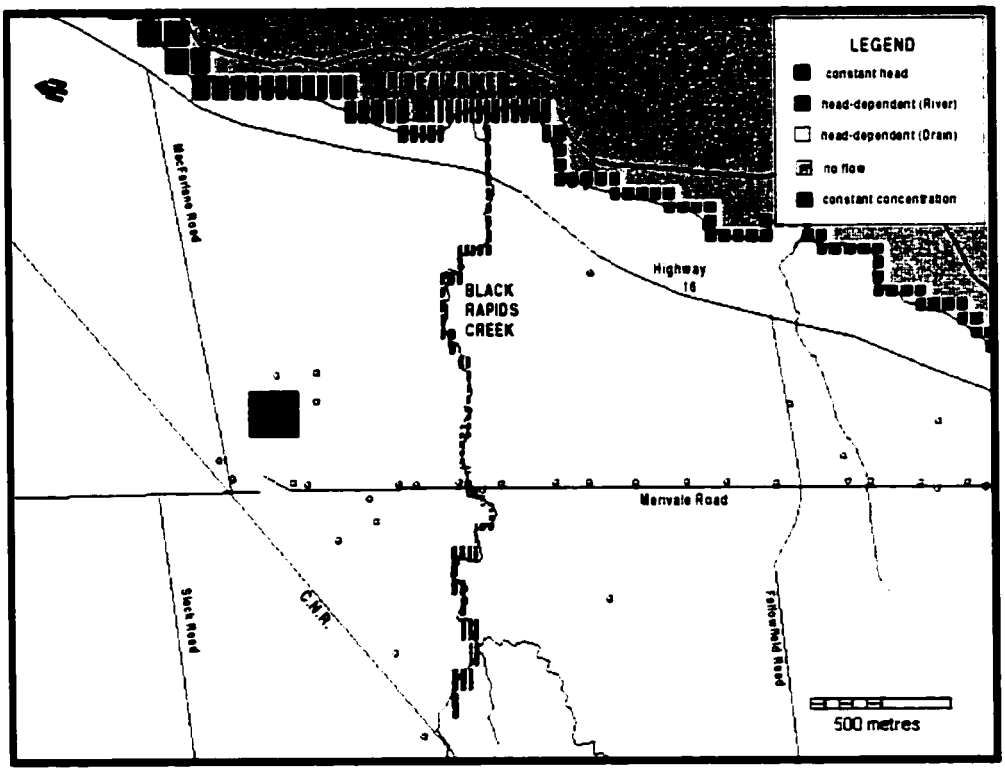

Figure 6B Boundary conditions – study area.

3.4.3 Head-Dependent Flow Boundaries

Head-dependent flow conditions allow flux across a boundary at a rate dependent upon the difference between a user-specified head (at the boundary), and the model calculated head adjacent to, or below, the boundary. In addition to the head difference, the flux, or rate of leakage, depends upon the vertical hydraulic conductivity of an interface material between the aquifer and the source (e.g. riverbed sediments) and the thickness of the interface material. These types of boundaries may be used to represent such physical features as lakes, rivers, streams, and drains (Anderson and Woessner, 1992).

Such features can be simulated with MODFLOW using the river, stream, or drain packages (subroutines). The river package allows water flow from the aquifer to river (or lake or stream) reaches which are gaining and vice versa where the river is losing. However, in this latter case, discharge from the river is independent of the river discharge. Thus, a losing reach could recharge the aquifer with more water than is being carried in the river (Anderson and Woessner, 1992). This problem is alleviated in the stream package, which allows leakage to and from the source in the same manner as the river package, but also considers the volume of streamflow in each river segment[4]. Thus streamflow will increase in areas of gaining reaches and decrease (and potentially go dry) in areas where the stream is losing. The drain package also works in much the same way as the river package, except that leakage

[4] Hence this parameter must be known or estimated for input to the model. Where it is not known or can not easily be estimated, use of the river package may be preferred.

from the drain to the aquifer is not allowed. When heads in the aquifer fall below the drain elevation, discharge to the drain will be zero (Anderson and Woessner, 1992).

With respect to this model, head-dependent flow boundaries were used to simulate the Rideau River, Black Rapids Creek, East Barrhaven Creek, and the tunnel.

Rideau River

The Rideau River formed the eastern boundary of the active portion of the model. River surface elevations range between approximately 75 and 78 m.a.s.l. across the study area. As stated in Section 2.3.2, the river partially penetrates the aquifer along most (if not all) of its length across the site. Preliminary modeling efforts were completed wherein this feature was simulated as a constant head boundary. However, the results of steady state simulations showed that the use of constant heads along this boundary exerted too strong an influence on the local flow system, depressing heads within the study area significantly lower than those actually observed, unless unrealistic values were used for parameters such as recharge and hydraulic conductivity. As a result, simulations were attempted wherein the river was represented as a head-dependent flow boundary using MODFLOW's river package. Since the results of these simulations were far more representative of observed conditions, modeling proceeded on this basis.

Jock River

The Jock River forms the southern boundary of the active portion of the model. Surface water elevations on the Jock River range between approximately 90 m.a.s.l. at the western

end of the model domain and 78 m.a.s.l where it flows into the Rideau River (Rideau Valley Conservation Authority, 1980). This feature was also simulated as a head-dependent flow (river) boundary.

Creeks

Portions of both Black Rapids Creek and the East Barrhaven Creek[5] (see Figure 6a) were also simulated as head-dependent flow boundaries. This could have been accomplished using either MODFLOW's river or stream package. Both of these creeks flow year round and are considered to be gaining under steady state conditions. The observation that Black Rapids Creek continued to flow even when it was no longer gaining (during periods of maximum drawdown associated with tunnel dewatering) indicated that the use of the river package was appropriate.

Since the East Barrhaven Creek was further removed from the area where dewatering was occurring, the choice of which package to use was of less significance. To the north, Nepean Creek was not simulated since no water level information was available in this area and since it was considered to be far enough removed from the study area to be of great significance.

Tunnel

The tunnel itself was simulated as a head dependent boundary using MODFLOW's drain package. Since the study was retrospective and dewatering rates were known, and since

heads were not lowered to the level of the tunnel, it could also have been simulated as a specified flux boundary. However, this would be conceptually inaccurate and furthermore it would not allow for the evaluation of the effectiveness of different tunnel grouting scenarios.

3.5 *Discretization of Time*

In order to effectively simulate transient dewatering impacts during tunnel construction, it was recognized that the model would need to account for the advance of the tunnel with time. For the length of tunnel simulated in this study (1,400 metres), dewatering occurred for a period of 176 days (i.e. the length of time it took to mine that distance). Since simulating dewatering over that entire distance for that period would certainly overestimate the tunnel's impact, it was clear that the 176 days would need to be broken down into a number of stress periods. In this way, only the northernmost portion of the tunnel would be simulated during the first stress period, and additional tunnel segments would be simulated with each new stress period.

Based upon the results of some preliminary transient simulations, it was determined that simulating the tunnel advance with seven stress periods would yield adequate results without requiring excessive computational time. Rather than discretizing time equally, the tunnel was broken down into seven equal lengths of 200 metres. On this basis, the length of stress

---

[5] The portions of the creeks simulated were based upon the relationship between the inferred creek bottom elevation and the inferred top of the till/bedrock unit (i.e. the creek boundaries were placed at nodes where the creek intersected the till sequence).

periods was based upon the actual length of time taken to mine each 200 metre section, as outlined below.

Table 1
Model Stress Periods

Stress Period No.	Length of Tunnel (m)	Cumulative Length of Time (days)
1	200	25
2	400	59
3	600	80
4	800	95
5	1,000	117
6	1,200	140
7	1,400	176

Each stress period was further discretized into 5 time steps, using a time step multiplier of 1.2 (i.e. MODFLOW increases the length of the time steps within each stress period as a geometric progression of ratio 1.2). The effects of varying the number of stress periods during model calibration is discussed in Section 4.2.3. The effect of varying the number of time steps per stress period was evaluated as part of the sensitivity analysis (Section 5.2).

3.6 Input Parameters

Model input parameters were selected based upon the following considerations:

- known or estimated aquifer properties alone (top and bottom elevations),
- trial and error calibration alone (porosity, riverbed conductivity, drain conductivity), or
- parameter values were varied within a known range or a range believed to be reasonable and set at the value which yielded the best calibration (hydraulic conductivity, storativity, recharge).

3.6.1 Hydraulic Conductivity

Aquifer hydraulic conductivity was inferred from transmissivity values calculated from design stage pumping test data (OMM, 1993a). As described in Section 2.3.3, transmissivity values calculated from two pumping tests conducted at locations along the tunnel alignment were quite consistent, with slightly higher values at locations along the northern part of the alignment (TW1 pump test).

Assuming an aquifer thickness of approximately 48 metres in the vicinity of TW1 (See section 3.6.2 below), the resulting hydraulic conductivities from the TW1 pump test ranged from 2.0 to 3.4 m/day and had an arithmetic mean of 2.2 m/day. Since this data was considered to be most representative of aquifer conditions along the portion of the tunnel to be simulated, the horizontally averaged hydraulic conductivity in this area was assumed to fall within this range. Furthermore, given the similar range of transmissivity values derived from the TW2 pumping test, this range was considered appropriate for the entire study area.

Based upon the observed vertical fracturing of the bedrock through which the tunnel was constructed, the horizontal hydraulic conductivity of the bedrock sequence was assumed to be anisotropic. As outlined previously, these vertical fractures were observed to be oriented more or less perpendicular to the tunnel alignment. As such, this anisotropy was easily simulated through setting K_y (the hydraulic conductivity component perpendicular to the tunnel) higher than K_x (the hydraulic conductivity component parallel to the tunnel). The degree of anisotropy was assessed through model calibration.

3.6.2 Top and Bottom Elevations

As described in Section 2.3.2, the available data concerning aquifer top elevations (i.e. the top of the till/bedrock unit) was contoured in order to provide a representation of the top surface of the aquifer (Figure 5). The output from the contouring software was input directly to the MODFLOW pre-processor to define the layer top elevations array. Based upon an assumed average top elevation of 80 m.a.s.l. and an average aquifer thickness of 44 metres[6], the bottom elevation was set at 36 m.a.s.l. for the entire model domain. These values were not varied during any of the simulations since it was determined that the aquifer transmissivity should remain consistent with the values discussed above.

3.6.3 Storativity

Calculated storativity values from design stage studies for the tunnel project (OMM, 1993a) ranged between approximately 1×10^{-4} and 3×10^{-3}. This range of values was considered appropriate for use with the model. Storativity values were varied within this range (for transient simulations) during model calibration.

3.6.4 Recharge

The magnitude of indirect recharge to the aquifer through downward flux from the overlying silts and clays was not known. A reasonable range for recharge values has been estimated by CCME (1996) at 0.005 to 0.5 m/year, with a modal value for the Windsor to Quebec City

---

[6] Assuming an average thickness of the Oxford Formation within the study area to be approximately 40 metres (see Section 2.1.2) and the average thickness of the till to be 4 metres.

corridor being 0.2 m/year. Consequently, recharge levels across the model domain were established through trial and error calibration of parameter values within this range.

3.6.5 Riverbed Conductance

The rate of leakage between river boundaries and the aquifer depends upon the relative head difference and the riverbed conductance. The riverbed conductance accounts for the spatial dimensions of the riverbed within the model cell, the thickness of the riverbed sediments, and their vertical hydraulic conductivity (McDonald and Harbaugh, 1988). The magnitude of these latter two parameters was not known with any degree of certainty for any of the modeled river boundaries. Consequently, this study assumed a fixed value for the thickness of the riverbed sediments (1 metre) and evaluated the vertical hydraulic conductivity of riverbed materials through trial and error calibration.

3.6.6 Drain Conductance

Similarly, the conductance of drain materials was not known. Since MODFLOW treats drain boundaries in a similar fashion to river boundaries, the same approach was utilized – a fixed value was assumed for drain bed thickness (1 metre) and the hydraulic conductivity of drain bed materials was established through trial and error calibration during transient (stressed) simulations. For this application, drain conductance was taken to represent the hydraulic conductivity contrast between the bedrock materials immediately adjacent to the open tunnel (drain) and the surrounding aquifer materials. This contrast in conductivity was assumed to be directly related to the effectiveness of grouting activities completed to control groundwater

inflows to the tunnel. Of note, the actual thickness of this grouted zone would be likely to extend out to at least one to two metres from the tunnel as a result of the grouting methodologies utilized.

3.6.7 Porosity

Since the porosity of the aquifer was not known with any certainty, the value of this parameter was established through model calibration. This was accomplished through simulating the observed movement of highly mineralized water (as represented by dissolved chloride) from an existing source area to a downgradient receptor (domestic well) as a result of tunnel dewatering. Since the approximate variation in chloride concentration with time was known at the downgradient receptor and since chloride acts as a conservative tracer (i.e. transport can be simulated through advection alone), porosity was varied until observed conditions were duplicated. This is discussed further in Section 4.2.2.

3.6.8 Initial Concentrations

For the purpose of simulating the migration of dissolved chloride from the identified source area (as defined in Section 3.4) towards the tunnel, an initial concentration of 50 mg/L was established over the entire model domain. Based upon the available water quality data, this concentration was considered to be representative of actual chloride concentrations measured at locations between the source area and the tunnel, which comprises the area of interest in terms of this aspect of the model.

4.0 Model Calibration and Verification

Model simulations were run using the boundary conditions discussed in Section 3.4 and initial parameter values based upon the considerations described in section 3.5. Steady state conditions were simulated as a first step, followed by simulation of stressed conditions (due to tunnel dewatering) using the steady state heads as initial values.

4.1 Steady State Conditions

4.1.1 Calibration Values

Steady state simulations were calibrated to observed head values as measured on June 6, 1996 (see Figure 4). A total of 37 calibration values were used (as shown on Figure 9 and compiled in Appendix B). As noted previously, the majority of this data comes from locations proximal to the tunnel axis. Therefore, simulated heads beyond the main study area were for the most part calibrated on a qualitative basis only, based upon factors such as the observed trend in the local groundwater gradient and surface elevations.

The main source of error associated with these calibration values is considered to result from the fact that the data points used consist of wells with differing screen lengths completed at different elevations within the aquifer. It was estimated that this variation would translate to point of measurement elevation differences of approximately 10 metres. As stated previously, the observed vertical gradient within the aquifer was determined to be approximately 0.04 m/m. Therefore, the point of measurement uncertainty would account for an error of approximately 0.4 metres in the hydraulic head calibration values. Allowing for

other potential sources of error (measurement error, transient effects, etc.), a total error of 0.5 metres in the hydraulic head calibration values was considered appropriate for use in the evaluation of simulation results. This 0.5 metre error is referred to hereafter as the '0.5 m. calibration value error level'.

4.1.2 Final Parameter Values

Calibration proceeded by trial and error using the parameter values or ranges of values described previously. Calibration followed an iterative process wherein steady state conditions were first simulated, followed by the attempted simulation of stressed conditions as observed during the TW1 pumping test described previously. Since the pumping test did not produce sufficient drawdowns at the monitoring locations to permit a quantitative evaluation of the model calibration, these stressed simulations were used as a qualitative check only. In this way, parameter values that produced a very significant difference between the calculated and observed responses could be modified, and the steady state simulation recalibrated.

The final parameter values utilized by the calibrated model are described below.

Hydraulic Conductivity

The closest steady state calibration resulted from the use of anisotropic hydraulic conductivity values of 1.0 m/day for K_x and 3.0 m/day for K_y across the entire domain. The average value of 2.0 m/day falls at the lower end of the range which was considered to be acceptable.

Recharge

The final recharge value used for the portions of the model comprising the study area was 9 x 10^{-4} m/day (0.33 m/year)[7]. This fell near the upper end of the range which was considered to be reasonable (0.005 to 0.5 m/year, modal value of 0.2 m/year). As noted previously, recharge in this model represents downward flux to the aquifer from the overlying silt/till unit. The possibility that this unit could be vertically discontinuous at some locations may support recharge values of this magnitude. In any event, the ultimate source of groundwater influx to the aquifer does not pose a large constraint with respect to this type of dewatering simulation.

This parameter, along with the riverbed conductivity along the Rideau River, proved to be the key factors in simulating the observed heads within the study area. Lower values of recharge and higher values of conductivity for the Rideau River tended to produce a more gradually

[7] Recharge values for the western portions of the model domain were significantly lower (0.02 – 0.11 m/year). Higher recharge values in this area resulted in unrealistically high heads. Alternatively, heads could have been controlled by specifying a lower head level at the western boundary (and consequently a lower flux from this boundary). However, the source of groundwater flux to or from the aquifer in this area was not considered to be an important issue for this study since it would not significantly impact the flow regime within the study area.

sloping potentiometric surface, resulting in calculated heads significantly lower than actually observed within the study area.

Riverbed Conductivity

For the Rideau River, the final hydraulic conductivity for riverbed materials was 3×10^{-3} m/day. Values of 1.0 m/day and 6.25 m/day were utilized for the Jock River and Black Rapids Creek, respectively. The relative difference between these latter two values and that for the Rideau River is considered to be consistent with the fact that both the Jock River (within the area modeled) and Black Rapids Creek represent higher energy environments (i.e. the riverbeds would consist of coarser, more conductive materials).

4.1.3 Relationship Between Observed and Calculated Heads

The final calibrated steady state solution shows a generally good agreement with the observed values within the study area. This conclusion is supported by the following lines of evidence:

1. The calculated distribution of heads for the calibrated steady state solution is shown as contour plots Figure 7a (entire model domain) and Figure 7b (study area). Visual comparison of Figure 7b to Figure 4 shows a good general correlation of head values and groundwater flow patterns.

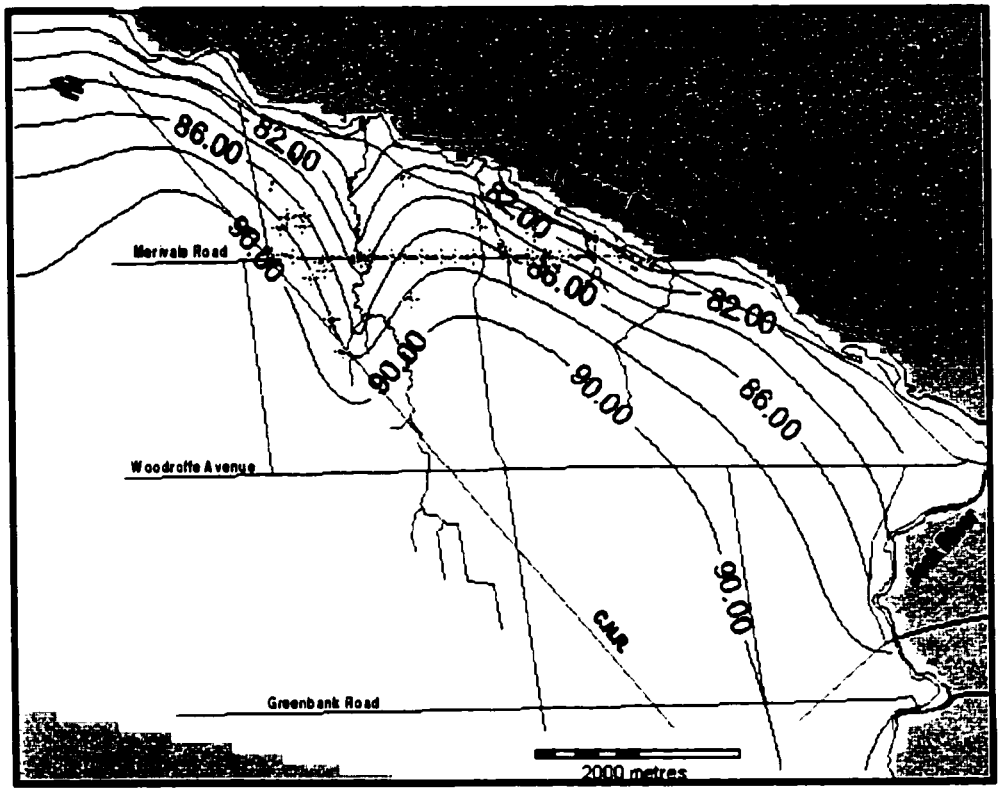

Figure 7a Simulated steady state head distribution – entire model domain

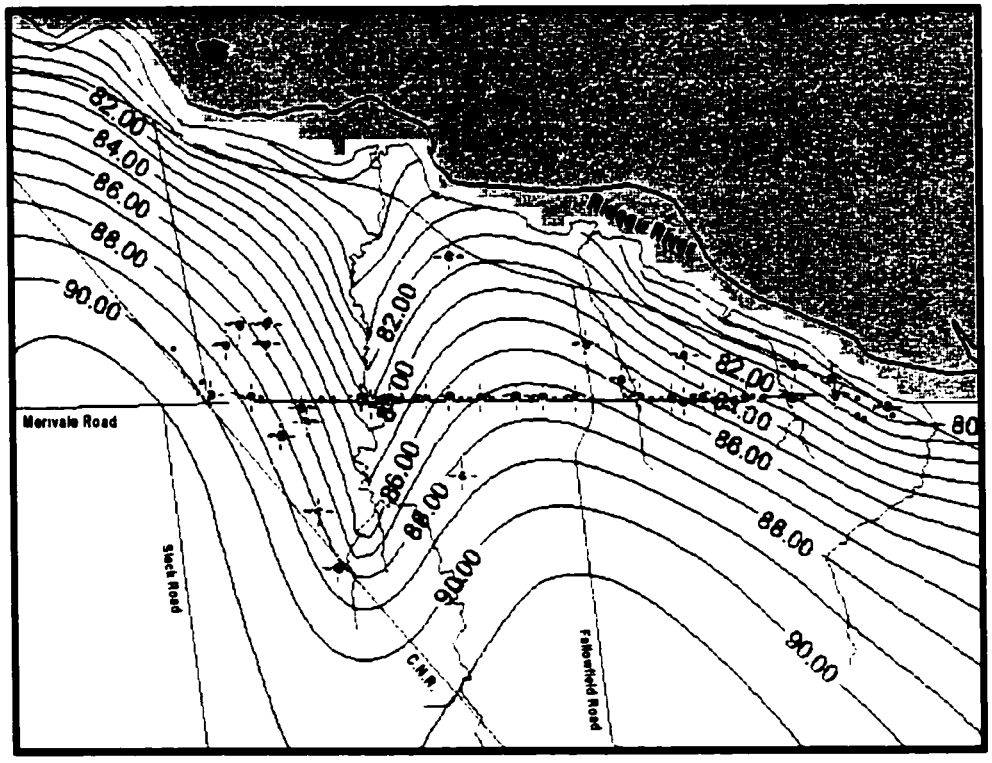

Figure 7b Simulated steady state head distribution – study area

2. Calculated heads at the target locations were plotted against the observed heads (calibration values) (Figure 8). This plot confirms that a relatively good calibration was obtained, as indicated by the data set's fit to the 45° line and the generally even distribution of data points on either side of the line.

Figure 8
Calculated vs. Observed Heads
Steady State Solution

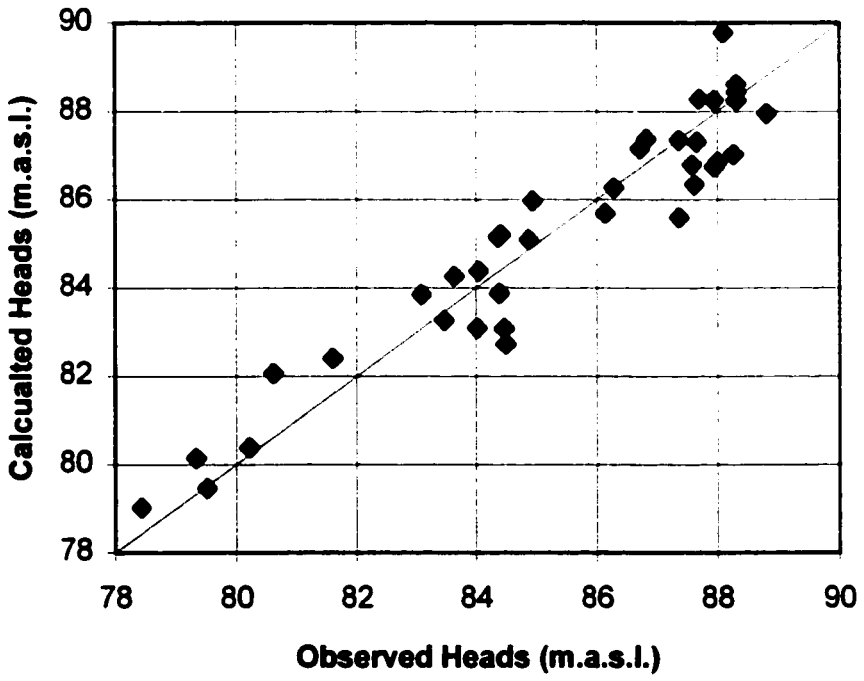

3. The average difference between the calculated and observed heads (residuals), expressed as the mean error was 0.04 m. The root mean squared error was 0.87 m. Also, the mean absolute error was 0.71 m. These three values serve to quantify the average error in the calibration. In all three cases, the average error levels are considered to be adequately low for the purpose of this study. This data is summarized in Table 2, below. Specific well locations are shown in Figures B1 and B2 (Appendix B).

Table 2
Calculated and Observed Heads for Steady State Solution
(all values in metres)

Target Name	Observed	Calculated	Residual	Target Name	Observed	Calculated	Residual
132 Grenfell	87.94	88.25	-0.31	Omm8	86.82	87.37	-0.55
75 Pineglen	88.80	87.95	0.85	R89-6	86.72	87.15	-0.43
Omm3	88.31	88.24	0.07	Omm10	84.36	85.15	-0.79
Omm4	88.00	86.85	1.15	Omm5	86.14	85.69	0.45
92-102	87.95	86.74	1.21	R89-7	84.93	85.97	-1.04
92-101	88.30	88.61	-0.31	TW2	84.40	85.20	-0.80
Omm1	87.70	88.28	-0.58	92-113	84.86	85.10	-0.24
Omm2	87.58	86.79	0.79	92-114	83.63	84.26	-0.63
4 Leeward	87.66	87.31	0.35	92-115	83.08	83.85	-0.77
28 Pineglen	86.28	86.26	0.02	Omm12	84.49	82.72	1.77
GB1	88.30	88.44	-0.14	Omm11	84.04	84.38	-0.34
93-103	84.01	83.09	0.92	95-2	80.61	82.06	-1.45
TW1	84.46	83.08	1.38	95-3	79.33	80.15	-0.82
R89-3	84.38	83.88	0.50	96-2	78.43	79.02	-0.59
Ruiter well	81.60	82.40	-0.80	94-6	80.21	80.38	-0.17
Omm7	87.36	85.60	1.76	Omm14	79.51	79.47	0.04
R89-4	87.62	86.33	1.29	94-1	83.47	83.27	0.20
92-108	88.26	87.02	1.24	85-7	88.09	89.78	-1.69
R89-5	87.36	87.35	0.01				

Mean Error	0.04
Root Mean Squared Error	0.87
Mean Absolute Error	0.71
Min. Residual	-1.69
Max. Residual	1.77
Head Range	10.37

4. Figure 9 shows the level of calibration obtained with respect to the specific calibration values (target heads) utilized. The level of calibration has been discretized into 0.5 metre increments of residual heads consistent with the calibration value error level defined in Section 4.1.1. As depicted on Figure 9, most of the study area was successfully calibrated to within two times the calibration value error level (as defined in Section 4.1.1). The remaining areas (where the calculated heads fell between two and four times the calibration value error level) were generally evenly distributed along the tunnel alignment, indicating that the calibration in these zones would be difficult to improve without adversely impacting upon the calibration in the adjoining (better calibrated) zones.

The final steady state calibration could have been improved through more localized parameter manipulation. However, this could not be supported based upon the available data relating to the physical and hydrogeological characteristics of the study area. For example, it was recognized that some anomalies in the observed head distribution (see Section 2.3.1) likely reflected differences in elevation head between monitoring locations (in the presence of a downward vertical gradient). As such, parameter manipulation to produce better agreement with observed data was not considered justified. Furthermore, given the level of calibration obtained, additional improvement was not considered necessary for the purposes of this study.

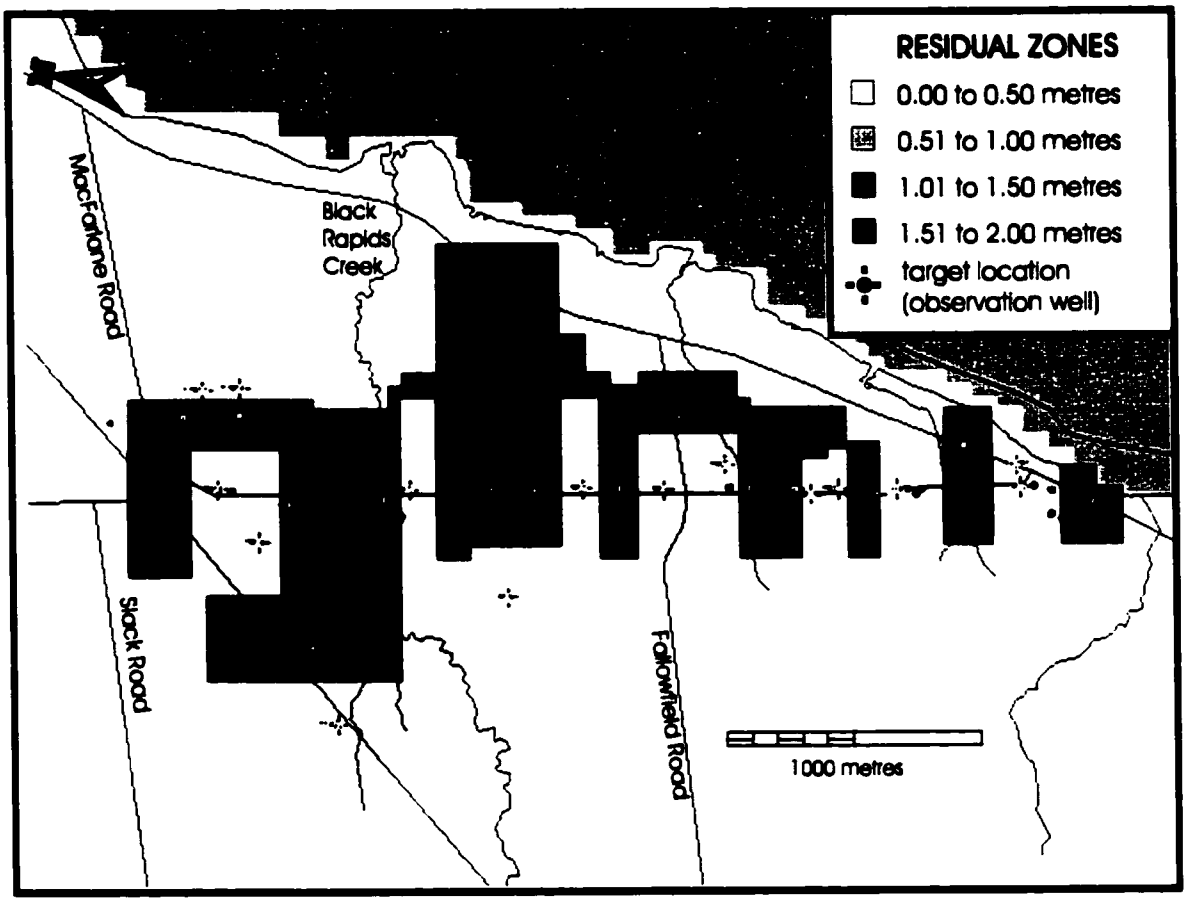

Figure 9 Diagrammatic representation of level of calibration obtained for the steady state simulation. Residual zones indicated correspond to approximate areas where the difference between calculated heads and target heads falls within 1, 2, 3, and 4 times the calibration value error level. Of note, the zones with higher residuals are generally dispersed between areas with lower residuals along the tunnel alignment. It is also noted that most of the target locations further removed from the tunnel alignment had relatively low residual values.

4.1.4 Water Balance

The water balance for the calibrated steady state solution had a small mass balance error of 0.10% (as outlined in Table 3, below). Anderson and Woessner (1992) state that a mass balance error of less than 1% is generally considered acceptable.

Table 3
Mass Balance – Steady State Solution

Boundary	Inflow (m^3)	Outflow (m^3)
Storage	0	0
Constant Head	0	663.45
Recharge	15,910	0
River Leakage	453	15,715
Total	16,363	16,378
	Inflow – outflow	-16.062
	Mass Balance Error	-0.10%

4.2 Stressed Conditions

4.2.1 Calibration Values

Transient (stressed) simulations were calibrated to head changes (drawdown) observed at monitoring locations during tunnel construction and to average pumping rates from the tunnel.

In terms of the error level associated with drawdown measurements, there were considered to be two main sources of error:

1. Firstly, despite the strong component of horizontal flow induced by tunnel dewatering, data from multi-level monitoring wells completed within the till/bedrock unit generally continued to show a similar vertical gradient to that observed under steady state conditions (i.e. approximately 0.04 m/m). Again, this would translate to a hydraulic head (and drawdown) error level of approximately 0.4 m for this factor alone.

2. Additionally, a significant seasonal influence on groundwater levels would be expected over a period of 176 days (i.e. unrelated to tunnel construction). As such, drawdown levels used as calibration values were adjusted to account for this influence based upon the observed seasonal fluctuations in groundwater levels in the area under steady state conditions (based upon both pre- and post-construction monitoring data). It is difficult to estimate the error level associated with this factor, however, it was judged to be likely to range between approximately 0.1 and 0.3 m.

Consequently, a larger error level was assumed to be associated with these drawdown measurements than with the steady state head level measurements. This error level was estimated to range from approximately 0.5 to 0.8 m.

Pumping rates from the tunnel were measured on a regular basis as either the time required to fill a known volume (earlier data), or as the head behind a calibrated v-notch weir (later data). The level of error associated with this latter method is likely to be on the order of 10% (Driscoll, 1986). The level of error associated with the former method is difficult to estimate, although it is certainly higher. Since the flow rates used as calibration values were averaged

over the period being simulated, the calibration error level would reflect errors associated with both methods. Allowing for other sources of error (e.g. reading error, water losses between the pumps and the measurement point, etc.), it was assumed that a reasonable error level for flow rate calibration values would be approximately 20%.

4.2.2 Final Parameter Values

Calibration of the transient simulations involved only those parameters not previously established through calibration of the steady state solution (storativity, drain conductance, porosity). Calibration for these parameters proceeded by trial and error.

The final parameter values utilized by the calibrated model are described below.

Storativity

Storativity was kept uniform across the entire model domain and varied within the range determined to be appropriate (1×10^{-4} to 3×10^{-3}). The best transient calibration resulted from the use of a uniform storativity value of 1.1×10^{-3}, which was equivalent to the arithmetic mean of the storativity values derived from the TW1 pumping test.

Drain Conductance

The hydraulic conductivity of drain materials (i.e. the zone of grouted bedrock encircling the tunnel) was varied through trial and error calibration until the best agreement with both observed drawdown and flow rates was obtained. This resulted in the use of hydraulic conductivity values of 0.15 m/day for portions of the tunnel north of Black Rapids Creek and

0.10 m/day for portions of the tunnel south of the creek. The implications of these values in terms of possible conclusions regarding the effectiveness of the grouting operations completed are discussed in Section 7.3.

Porosity

As outlined previously, porosity was calibrated through the simulation of the migration of dissolved chloride from an existing source area to a downgradient receptor well. This involved modeling the advective transport of chloride (using MT3D) within the calibrated transient flow system. Consequently porosity was the last parameter to be assessed. A contour plot of the calculated distribution of chloride concentrations is shown as Figure 10.

As depicted on Figure 10, the receptor well was located between the source area and the tunnel. This particular well was chosen as the receptor due to the fact that it was the best characterized in terms of water quality changes with time and represented the only location with sufficient data to support this type of modeling for the period of time simulated by the flow model. The observed chloride concentration at the receptor well near the end of the period simulated (i.e. 176 days) was 110 mg/L (having increased from approximately 50 mg/L). This value was best simulated using a porosity of 2%[8]. Based upon the simulated gradient between the receptor and the source, and a hydraulic conductivity of 2.0 m/day, the resulting advective velocity would be approximately 0.8 m/day, or 290 m/year.

[8] Literature values for the porosity of dolomitic bedrock range from 0-20% (Freeze and Cherry, 1979).

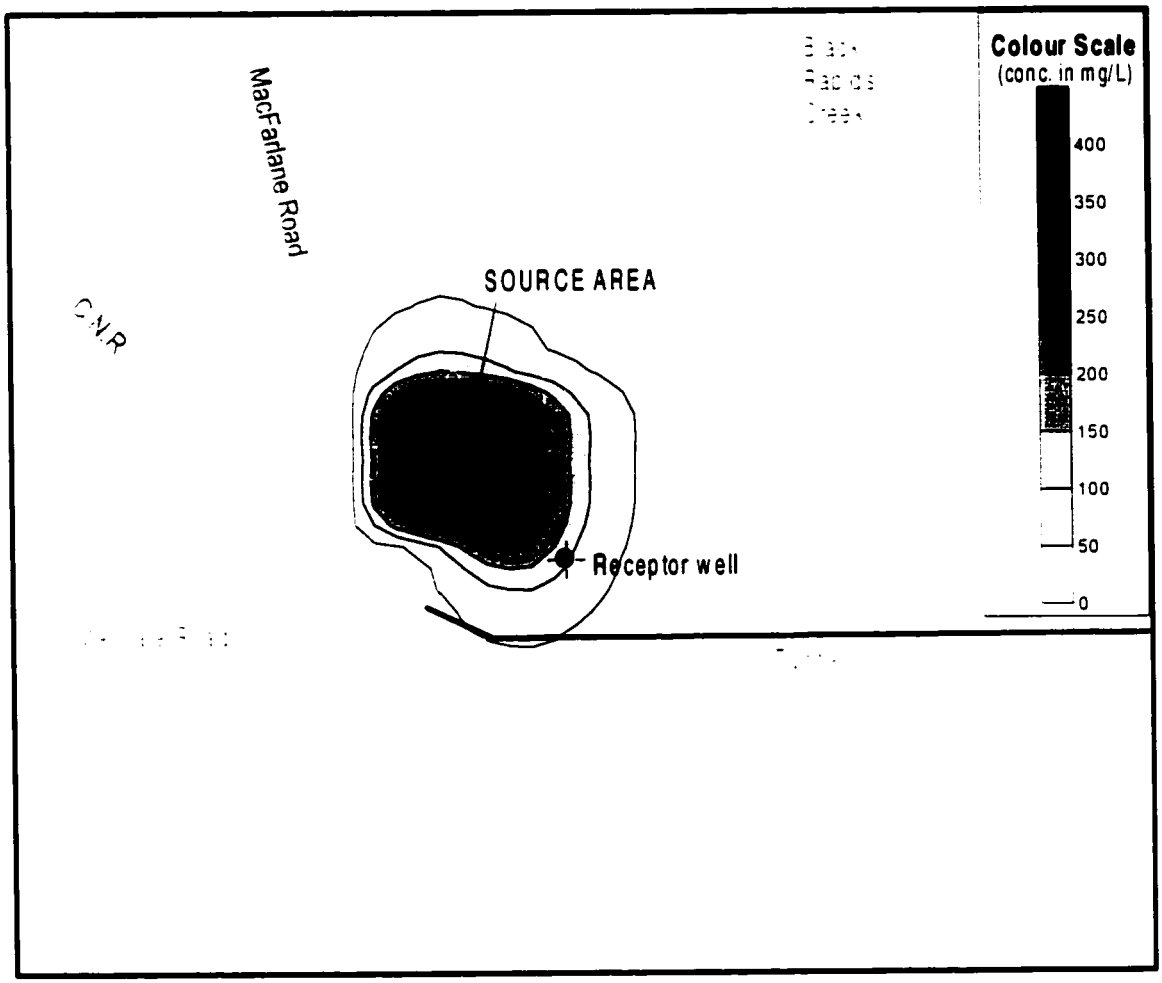

Figure 10 Simulated distribution of dissolved chloride concentrations after 176 days of tunnel dewatering. Advective transport of dissolved chloride within the stressed flow system was simulated with MT3D using an aquifer porosity of 2%, as calibrated to the observed chloride impact at a receptor well located between the tunnel and a known source area.

4.2.3 Relationship Between Observed and Calculated Drawdown/Flow

Figures 11a, 12a and 13a show contour plots of the simulated drawdown after 400, 800, and 1,400 metres of tunnel mining, respectively. These three plots show the progressive impact due to tunnel dewatering. Drawdown residuals at monitoring well locations adjacent to the active portions of the tunnel are also shown as insets on each of these figures.

A summary of the average statistics for the drawdown residuals at the end of each stress period is presented in Table 4.

Table 4
Average Error – Drawdown Residuals

Length of tunnel simulated (m)	Stress Period	No. of targets	Mean Error	Root Mean Squared Error	Mean Absolute Error
200	1	8	1.23	0.73	1.23
400	2	16	0.59	0.87	0.80
600	3	24	0.37	0.84	0.69
800	4	38	0.28	0.72	0.56
1000	5	52	0.44	0.88	0.65
1200	6	66	0.55	0.93	0.72
1400	7	82	0.59	0.95	0.76

Assuming a calibration value error level (drawdown) of 0.5 to 0.8 m. as discussed in Section 4.2.1, it can be seen that the majority of the statistics presented in Table 4 fall within this range, and all of the statistics fall within two times this range. This was considered to represent an adequate level of calibration to drawdown given the purposes of this study.

An assessment of the level of model calibration attained is also provided by Figures 11b, 12b, and 13b, which present graphs of the calculated drawdowns plotted against observed drawdowns at the target locations. These graphs show that the calculated values generally trend along the 45° line. It is noted that a number of points deviate significantly from this line, and generally show that drawdown was under-predicted relative to that observed. This reflects the fact that these simulations were calibrated to both drawdown and flow rates, since parameter variations which improved the calibration to drawdown resulted in a poorer calibration to flow rates. It is possible that the relatively high modeled recharge levels have contributed to this problem.

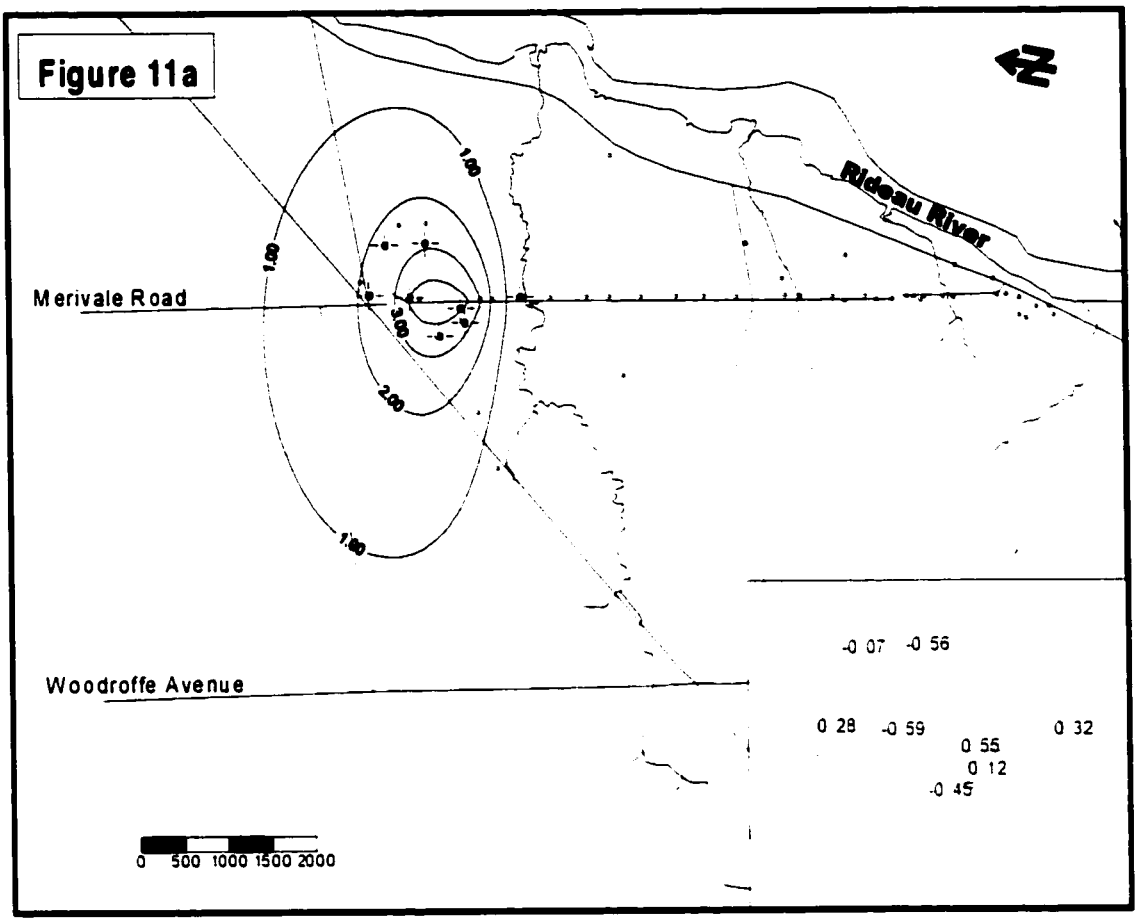

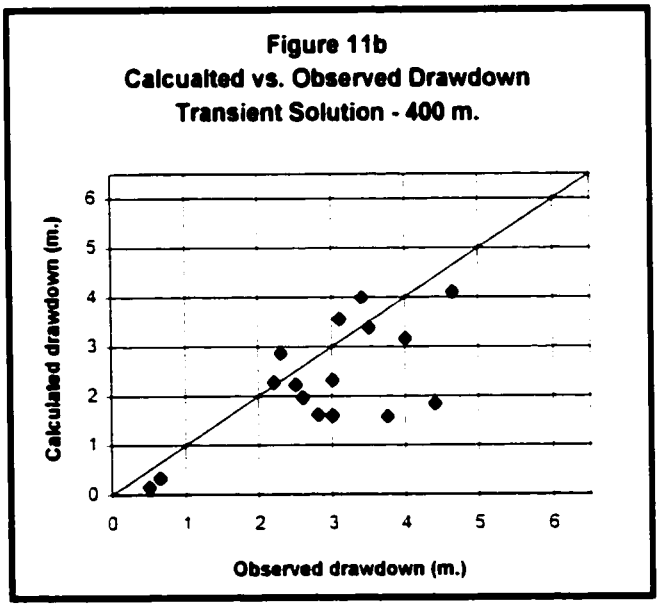

Figure 11 – Contour plot showing distribution of simulated drawdown after 400 metres of tunnel mining (Figure 11a). Residual values at the target locations are shown in the inset (for the last stress period). Figure 11b presents a scatter plot of calculated vs. observed drawdowns for all target locations up to the end of the same stress period.

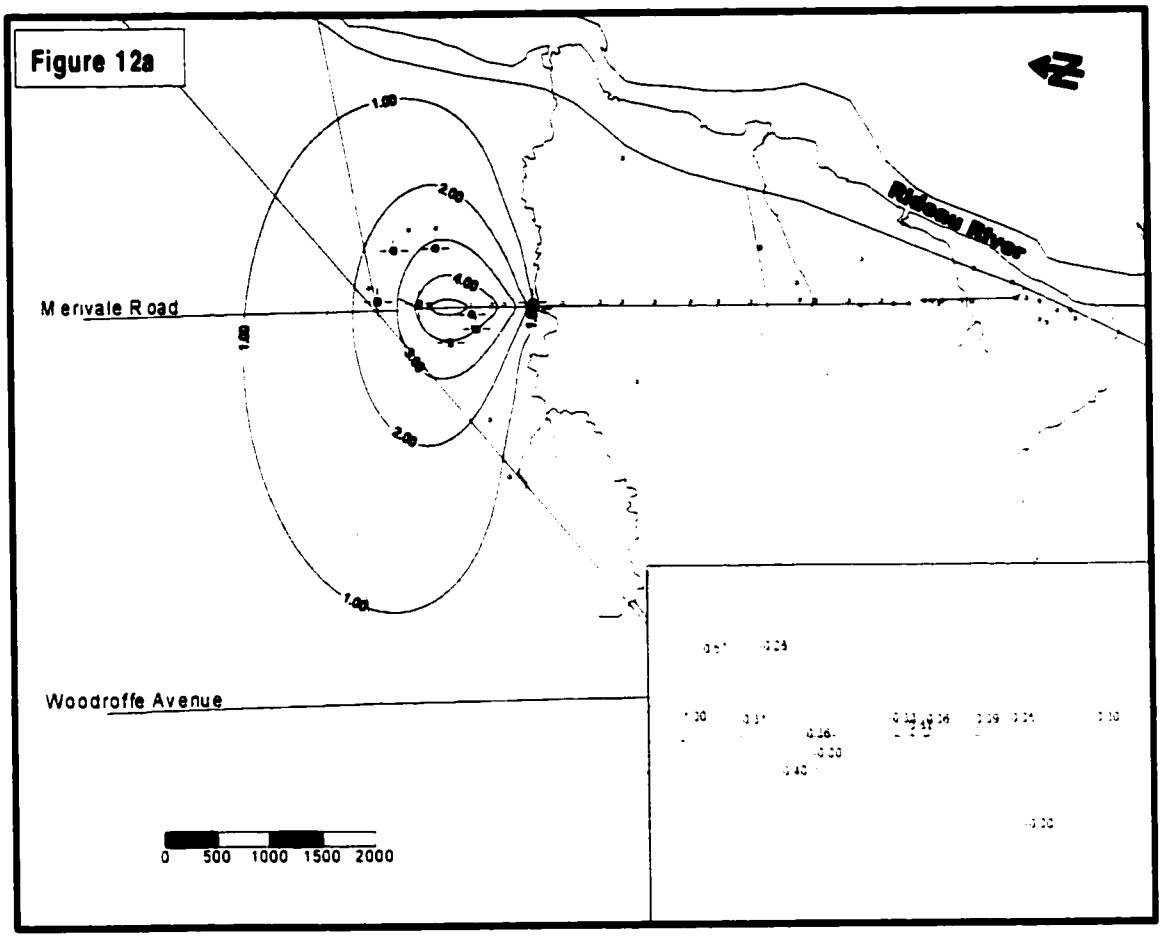

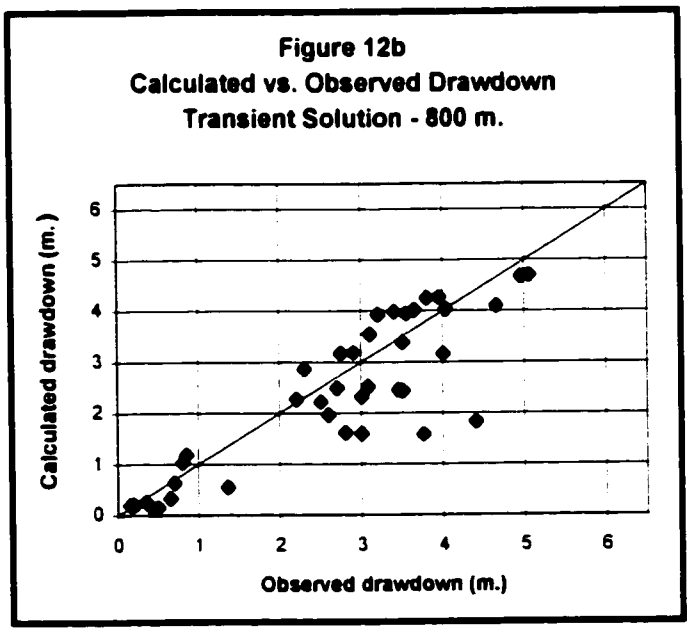

Figure 12 - Contour plot showing distribution of simulated drawdown after 800 metres of tunnel mining (Figure 12a). Residual values at the target locations are shown in the inset (for the last stress period). Figure 12b presents a scatter plot of calculated vs. observed drawdowns for all target locations up to the end of the same stress period.

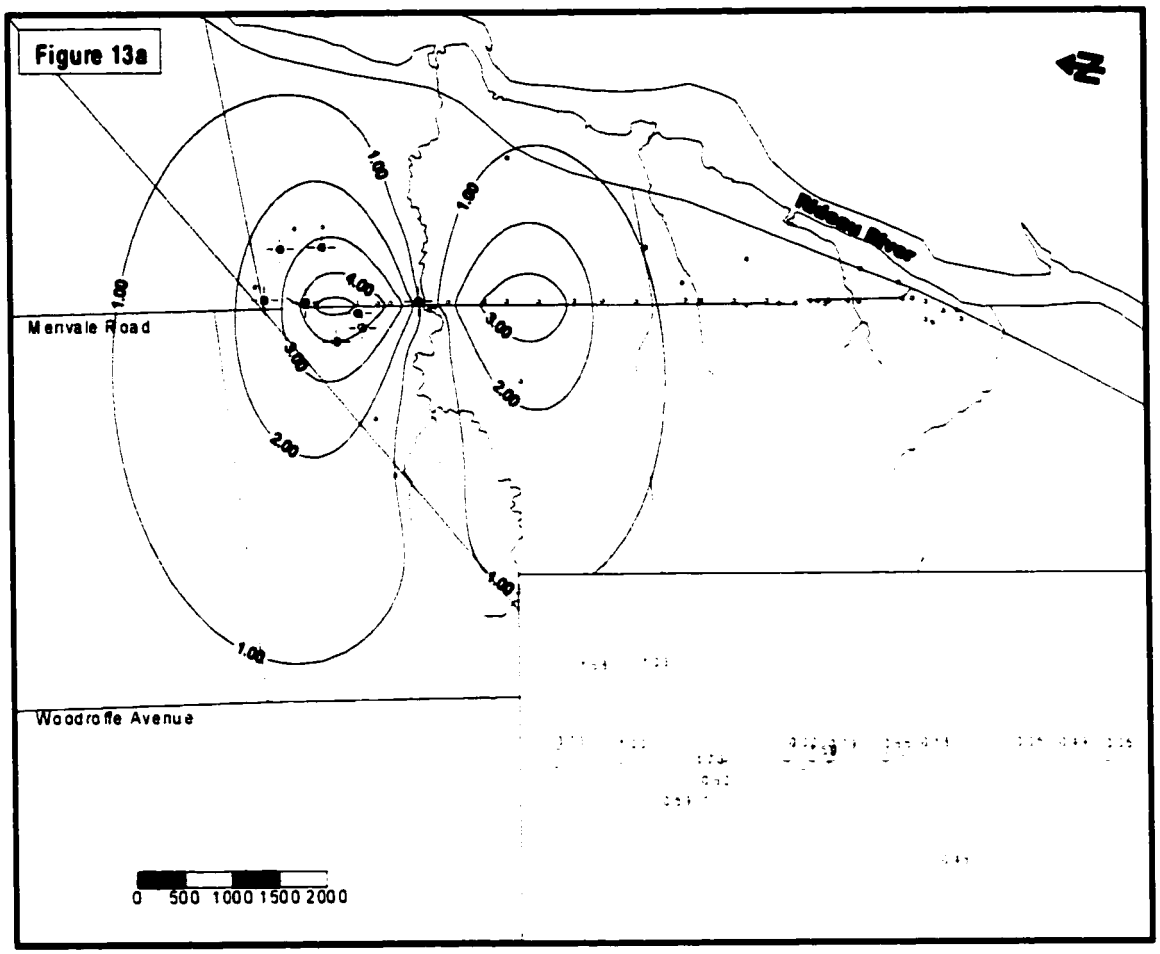

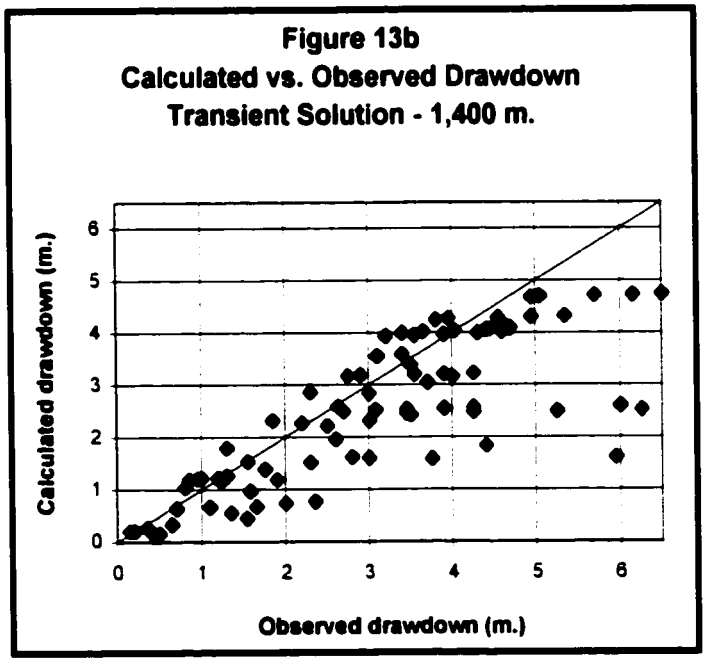

Figure 13 – Contour plot showing distribution of simulated drawdown after 1,400 metres of tunnel mining (Figure 13a). Residual values at the target locations are shown in the inset (for the last stress period). Figure 13b presents a scatter plot of calculated vs. observed drawdowns for all target locations up to the end of the same stress period.

As indicated previously, transient modeling proceeded with the tunnel being broken down into seven equal lengths of 200 metres. However, an evaluation was also undertaken of the effect on the model calibration of breaking the tunnel down into different lengths. This consisted of modeling the tunnel as two equal lengths of 700 metres (i.e. 2 stress periods), and as fourteen equal lengths of 100 metres (i.e. 14 stress periods), in addition to the baseline case of seven equal lengths of 200 metres (7 stress periods). While it is intuitive that increasing the number of stress periods (and the discretization of the tunnel advance) would more realistically simulate tunnel mining, it was considered instructive to quantify this effect.

In terms of drawdown, the effect of increasing the number of stress periods was small, with the drawdown cone only retracting slightly between each successive simulation (2, 7, and 14 stress periods). This is not considered to be surprising since the rate of tunnel advance (average of 8 m/day) was sufficiently slow to allow the aquifer's response to become asymptotic (approaching a steady state response to the applied stress). Consequently, it is clear that the effect of increasing the number of stress periods would only have a marginal effect on the drawdown cone, particularly adjacent to portions of the tunnel mined during earlier portions of the simulation.

With respect to flow rates (outflow from the tunnel), the effect was more significant. The calculated flow rates for different tunnel lengths using the 2, 7 and 14 stress period simulations are presented in Table 5.

Table 5
Flow Rates

Length of tunnel simulated (m)	Number of Stress Periods	Target Rate (L/min)	Simulated Rate (L/min)	% error
400	2 of 7	523	614	17
	4 of 14	523	534	2
800	4 of 7	642	814	27
	8 of 14	642	716	12
1400	2 of 2	810	1,491	84
	7 of 7	810	1,224	51
	14 of 14	810	1,065	32

As can be seen, outflow from the tunnel was over-predicted in all cases, with the level of error increasing as longer tunnel segments were simulated. The simulated flow rates per unit length of tunnel for all simulations ranged from approximately 0.8 to 2.2 L/min/metre of tunnel compared to the observed range of flow rates of approximately 0.6 to 2.1 L/min/metre of tunnel. In this sense, even the simulation with only 2 stress periods provided a reasonable estimate of outflow compared to the estimated rates using the Goodman[9] approach as described in Section 1.2.1. The database of observed flow rates is included in Appendix B.

[9] Flow rates of approximately 6 to 100 L/min/metre of tunnel were predicted during design stage studies for the tunnel (OMM, 1993a). Applying the hydraulic conductivity value of 2.0 m/day as modeled in this study would yield an estimated flow rate of 38 L/min/metre of tunnel.

4.2.4 Water Balance

The water balance for the calibrated transient solution (7 stress periods) had a very small mass balance error of 0.01% (as outlined in Table 6, below).

Table 6
Mass Balance – Transient Solution

Boundary	Inflow (m^3)	Outflow (m^3)
Storage	26,149	6.12
Constant Head	0	1.01×10^5
Drains	0	3.10×10^5
Recharge	2.80×10^6	0
River Leakage	1.10×10^5	2.53×10^6
Total	2.94×10^6	2.94×10^6
	Inflow – outflow	-210.25
	Mass Balance Error	-0.01%

5.0 Sensitivity Analysis

In order to assess the level of uncertainty in the model (steady state and transient), a sensitivity analysis was undertaken. This analysis consisted of assessing the model's response to changes in aquifer parameters, boundary conditions, and time discretization.

5.1 Steady State Solution

The steady state solution was subjected to systematic changes in parameter values for hydraulic conductivity of aquifer materials, recharge, and the hydraulic conductivity of riverbed materials (along river boundaries). The results of this analysis are presented in Table 7.

Table 7
Sensitivity Analysis – Steady State Conditions

Parameter	Parameter Variation	Mean Error		Root Mean Squared Error		Mean Absolute Error		Effect
	(% change)	(m)	(change)	(m)	(change)	(m)	(change)	
Base	0	0.04	--	0.87	--	0.71	--	--
Hydraulic Conductivity ($K_{aquifer}$)	+20%	0.73	1725%	0.84	3%	0.89	25%	Small
	+50%	1.41	3425%	0.93	7%	1.48	108%	Moderate
	+70%	1.74	4250%	1.0	15%	1.78	151%	Moderate
Recharge (r)	+20%	-0.73	1925%	1.01	16%	1.07	51%	Moderate
	-20%	0.82	1950%	0.86	1%	0.95	34%	Small
	+50%	-1.89	4825%	1.37	57%	2.01	183%	Large
	-50%	1.98	4850%	1.09	25%	2	182%	Large
Riverbed Conductivity (K_{river})	+100%	0.43	975%	0.87	0%	0.75	6%	Minimal
	-100%	-0.6	1600%	0.97	11%	0.96	35%	Small
	+500%	0.71	1675%	0.89	2%	0.93	31%	Small
	-500%	-2.04	5200%	1.45	67%	2.08	193%	Large

Hydraulic conductivity values were varied within the range previously determined to be appropriate based upon the results of pumping test analysis (2.0 to 3.4 m/day). Since the calibrated solution used a horizontally averaged hydraulic conductivity of 2.0 m/day, this resulted in a variation of up to 70%. As shown in table 7, values within the upper portions of this range (e.g. +50%, +70%) resulted in increases in calibration value error levels which were significant, although not excessive. As such, the calibrated steady state solution is considered to be moderately sensitive to changes in aquifer hydraulic conductivity. This fact is tempered however by the fact that the calibrated average aquifer hyudraulic conductivity more closely corresponded to the mean value of 2.2 m/day determined from the TW1 pumping test.

Since both recharge and the hydraulic conductivity of riverbed materials were established through calibration, these parameters were varied by sufficient magnitudes to cause significant effects. Based upon this analysis, the calibrated steady state solution is considered to be quite sensitive to changes in recharge rates, and less sensitive to changes in the hydraulic conductivity of riverbed materials.

5.2 Transient Solution

The transient solution (seven stress periods) was subjected to systematic changes in parameter values for storativity and the hydraulic conductivity of drain materials (zone of grouted rock in the vicinity of the tunnel). The results of this analysis are presented in Table 8.

Table 8
Sensitivity Analysis – Stressed Conditions

Parameter	Parameter Variation (% change)	Mean Error		Root Mean Squared Error		Mean Absolute Error		Flow Rate (L/min)	Effect
		(m)	(change)	(m)	(change)	(m)	(change)		
Base	0	0.59	--	0.95	--	0.76	--	1,224	--
Drain Conductivity (K_{drain})	+20%	0.28	53%	0.97	2%	0.69	9%	1,385	Small
	-20%	0.94	59%	0.96	1%	0.97	28%	1,077	Small
	+50%	-0.12	120%	1.03	8%	0.79	4%	1,594	Moderate
	-50%	1.56	164%	1.06	12%	1.56	105%	750	Moderate
Storativity (S)	+100%	0.64	8%	0.96	1%	0.79	4%	1,261	Minimal
	-100%	0.58	2%	0.95	0%	0.75	1%	1,227	Minimal
	+500%	0.77	31%	0.96	1%	0.86	13%	1,310	Small
	-500%	0.57	3%	0.95	0%	0.75	1%	1,221	Minimal

Based upon the results of this analysis as presented in Table 8, the calibrated transient solution is considered to be fairly sensitive to changes in the hydraulic conductivity of drain materials and not very sensitive to changes in storativity.

In addition to the parameters discussed above, an evaluation of the effect of varying the number of time steps per stress period was also completed. As outlined in Section 3.5, five time steps per stress period were utilized in this model. However, it was found that varying the number of time steps to as low as two per stress period resulted in no significant changes to the model solution.

6.0 Predictions

As discussed in Section 4.1.3 and 4.2.3, an acceptable level of calibration was considered to have been achieved for the purposes of this study. Consequently, the calibrated model was subsequently utilized for prediction of the effects of alternate tunnel construction scenarios as represented by varying model stresses during transient simulations. Specifically, the following scenarios were simulated:

1. tunnel mining with no grouting to control groundwater inflow (i.e. $K_{drain} = K_{aquifer}$),
2. tunnel mining with a faster advance rate (with K_{drain} at calibrated level),
3. tunnel mining with more effective grouting (lower K_{drain}), and
4. addition of artificial aquifer recharge using injection wells (with K_{drain} at calibrated level).

Additional details regarding the modifications to the model made for each of these scenarios, and the results obtained are provided hereafter.

Scenario 1 (tunnel mining with no grouting to control groundwater inflow)

This simulation involved modifying the hydraulic conductivity of the drain materials so that it was equal to the horizontally averaged hydraulic conductivity of the aquifer materials. No other parameters were varied.

Figure 14 shows the results of this simulation in terms of drawdown contours. Comparison of this figure to Figure 13, reveals that the impact of tunnel dewatering under these

conditions would be significantly greater. Had drawdowns of this magnitude been experienced, it is certain that the number of well interference problems occurring would have risen sharply.

The simulated pumping rate for this scenario was approximately 4,500 L/min., an increase of nearly 4 times compared to the calibrated simulation of actual conditions. Of note, the calculated head along the tunnel alignment was lowered to the tunnel invert during this simulation.

Scenario 2 (tunnel mining with a faster advance rate)

For this simulation all stress periods were set at 15 days, consistent with the fastest observed mining rate for a 200 metre length of tunnel (approximately 13 metres/day). The results of this simulation showed no significant differences compared to the calibrated simulation of actual conditions.

Furthermore, through correlating the actual timing of well interference problems with observed water levels at monitoring well locations, it was possible to determine what level of drawdown could be tolerated without causing any significant impact (in terms of well interference). Using this information and progressively decreasing the length of the stress periods, it was determined that even had the entire 1,400 metres of tunnel been mined in one day, some well interference problems would still have been likely (albeit a smaller number). As such, it can be concluded that the length of time required for tunnel mining was not a significant factor in terms of the observed impacts.

Scenario 3 (tunnel mining with more effective grouting)

As with scenario 2, this simulation involved a variation in the applied stress to determine what parameter value would result in no significant tunnel impact. In this case, the parameter varied consisted of the hydraulic conductivity of drain materials (K_{drain}).

It is noted that the calibrated simulation of actual conditions employed an average K_{drain} of approximately 0.12 m/day. This is approximately 17 times lower than the horizontally averaged $K_{aquifer}$. By progressively decreasing K_{drain}, it was determined that no significant well interference problems would have been likely had there been a contrast of approximately 40 times between the hydraulic conductivities of the aquifer and the rock mass immediately surrounding the tunnel (i.e. K_{drain} of 0.05 m/day).

Scenario 4 (addition of artificial aquifer recharge using injection wells)

Another method which could have been utilized to limit the impact of tunnel dewatering is the addition of artificial aquifer recharge using injection wells.

In order to evaluate whether this method could have been effective, model simulations were run with three injection wells located along the tunnel alignment north of Black Rapids Creek. The three wells were placed at locations where a suitable amount of publicly owned or controlled space was available (e.g. within the occupancy easement for the MacFarlane Access Shaft, on portions of the Regional road allowance not abutting private frontage), since this would have actually restricted where such wells could be placed.

Simulations were run using progressively higher injection rates until dewatering impacts were mitigated to the point that well interference problems would likely have been minimized. Such conditions were predicted using injection rates of 150 L/min. for the northernmost and southernmost injection wells, and 250 L/min. for the central well (Figure 16). Given the characteristics of the aquifer, these injection rates would likely have been realistically attainable.

Please note that K_{drain} was not modified during these simulations. As such, this scenario simulates the control of tunnel dewatering impacts through both grouting and injection.

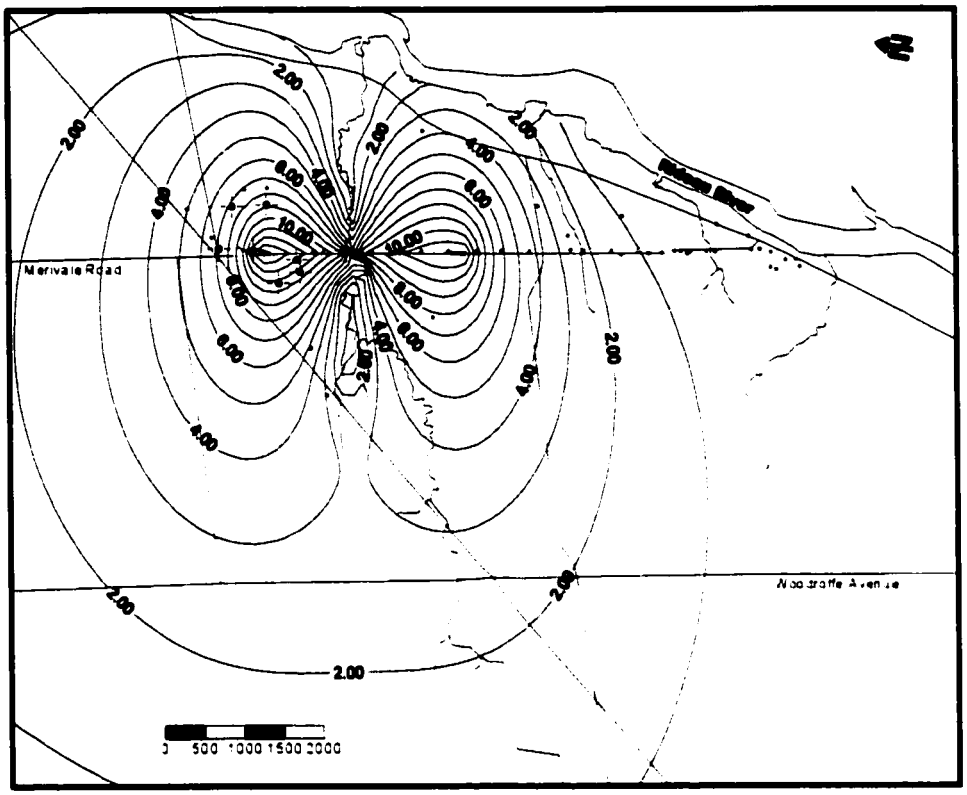

Figure 14 Simulated drawdown for scenario 1 ($K_{drain} = K_{aquifer}$)

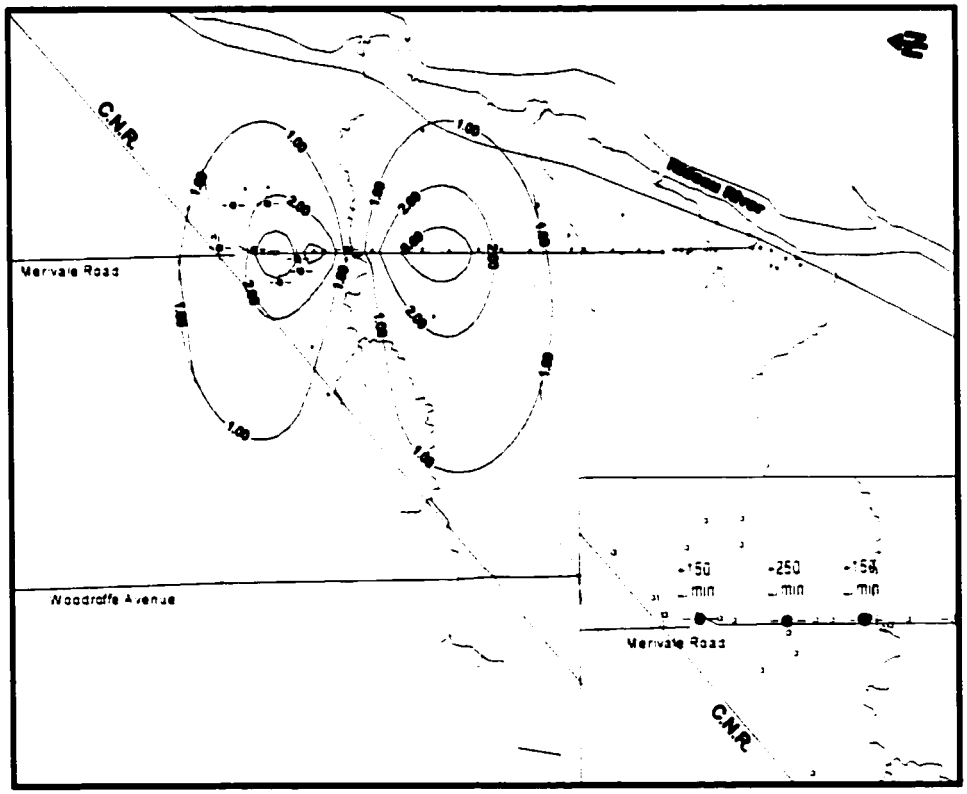

Figure 15 Simulated drawdown for scenario 4 (injection wells)

7.0 Discussion

7.1 Study Objectives

The objectives of this study, as outlined in Section 1.1, are summarized as follows:

- improve understanding of local groundwater flow regime;
- determine whether tunnel dewatering impacts could be effectively simulated using standard numerical groundwater flow modeling techniques, specifically addressing the following considerations:
  - the means of simulating an open tunnel both spatially and temporally (tunnel advance with time),
  - the use of an equivalent porous medium approach;
- complete predictive simulations using calibrated model; and
- the simulation of geochemical impacts to the aquifer.

As outlined in the preceding sections of this thesis, all of these objectives were satisfied.

The most significant contribution of this study in terms of the understanding of the local groundwater flow regime was the confirmation that the shallow bedrock and overlying till act as one aquifer and consequently represent a single hydrostratigraphic unit. This was indicated by the response observed in monitoring wells completed within both sequences during the design stage pumping test of TW1 (OMM, 1993a), and confirmed through numerical simulation. As outlined in Section 3.3, the results of preliminary modeling

wherein these two sequences were treated as separate layers showed that the overall flow field within and between the two layers could be well simulated under steady state conditions, but not under stressed conditions (little or no response within the till to pumping from the bedrock). This led to the conclusion that treating these sequences as separate layers was inappropriate.

The model also confirmed that the dominant east-west trending fracture orientation within the bedrock at the site results in an anisotropic hydraulic conductivity tensor. The degree of anisotropy was best simulated using a K_x/K_y ratio of 1:3, where K_y is parallel to the dominant fracture orientation.

Based on the calibration results obtained, the model was found to be effective for simulating tunnel dewatering impacts, where the tunnel is represented as a drain that advances with time through the use of successive stress periods. While there were some deficiencies with the transient calibration, the overall calibrated solution was found to provide a sufficiently realistic simulation of the actual dewatering impacts observed to both validate the approach used and allow the use of the model for prediction (see following sections). Furthermore, the use of an equivalent porous medium approach does not appear to have been a significant limitation for this application, although it may have had some impact on the transient calibration (this is discussed further in Section 7.4).

7.2 Modeling Approach

The modeling approach used differed considerably from that used by previous researchers investigating tunnel dewatering issues. As discussed in Section 1.2, most previous studies addressed the problem from what has been characterized herein as an 'engineering' perspective. By this it is meant that the studies focussed on predicting rates of groundwater inflow to a tunnel for the purpose of designing or assessing groundwater control techniques in order to facilitate tunnel construction, or even allow tunnel construction to occur. A review of these modeling techniques revealed that they generally do not attempt to characterize the flow system within which the tunnel is constructed. Furthermore, they were found to be of limited use for the problem at hand either because they require the use of fairly restrictive assumptions (e.g. Goodman et al., 1965), or because their focus was too heavily weighted towards the effects of groundwater inflows at the tunnel face (e.g. Anagnostou, 1995).

The one previous study in the available literature which addressed the problem from more of a hydrogeological (or flow system) perspective (Schweiger et al., 1993) also differed considerably from the approach used for this study. In that study, the approach consisted of the use of predictive modeling techniques to assess inflows both at the tunnel face and along the tunnel axis behind the face. These predicted flow rates were then used to establish a horizontal groundwater flow model wherein the tunnel was simulated as a constant flux boundary with flow rates changing with time as the tunnel advanced.

The results of this study suggest that when evaluating tunnel dewatering impacts from a flow system perspective, it is not necessary to assess groundwater inflow at the tunnel face as a separate issue, or even to quantify it at all. This stems from the fact that the tunnel acts as a drain and the tunnel advance rates are sufficiently slow that the drawdown response approaches steady state on a shorter time scale than both the advance of the tunnel and the subsequent installation of an impermeable liner. Consequently, even simulating the tunnel with a relatively small number of stress periods (i.e. simulating the tunnel advance as large segments per unit time) still yielded relatively good calibrations with respect to both simulated drawdown and flow rates. It is anticipated that this conclusion would be valid for the modeling of tunnels constructed through most types of geologic materials, but with the possible exception of very impermeable materials, where drawdown response times would be significantly longer (in such cases dewatering would be less of an issue, and as such modeling likely would not be completed anyway).

Having said this, the approach utilized herein could also be adapted for predicting groundwater inflows at the tunnel face simply through applying smaller discretizations both spatially and temporally to the leading edge of the tunnel. Considering MODFLOW specifically, a single cell or small range of cells at the leading edge of the tunnel could be specified as a separate drain reach which is active during only the last stress period. The rate of groundwater inflow to that cell (or range of cells) could then be computed for any desired length of time.

It is clear that for this approach to be valid, the model must reasonably represent the flow system within which the tunnel is constructed (it could however be argued that the same limitation exists for other approaches).

7.3 Project Specific Implications

With respect to the project that formed the basis of this study (the West Rideau Collector Sewer tunnel), the study results provide some insight into the effectiveness of the groundwater control procedures implemented, as well as the types of conditions that might have mitigated the impacts which occurred.

As outlined in Section 1.3, the groundwater control procedures implemented for this project consisted of grouting the rock mass surrounding the tunnel through both advance grouting from the ground surface and grouting from within the tunnel. Since there is no means by which a model such as this can distinguish between the effects of grout introduced via these two methods, only an evaluation of the sum total of these grouting efforts can be made. This evaluation assumes that the effects of these grouting efforts can be directly correlated to the contrast in hydraulic conductivity between the aquifer materials ($K_{aquifer}$) and the drain materials (K_{drain}), as determined by the calibrated transient solution.

As stated previously, the calibrated solution used a value for K_{drain} which was approximately 17 times lower than that of $K_{aquifer}$. Predicting the results when this contrast was eliminated (scenario 1) resulted in a significantly greater impact to the aquifer, with heads along the tunnel axis being lowered to the level of the tunnel invert. This suggests that the actual

grouting efforts completed significantly mitigated the well interference problems that might otherwise have occurred. It was also determined that lowering K_{drain} by a factor of approximately 40 times relative to $K_{aquifer}$ would likely have eliminated well interference problems altogether.

At first glance, the validity of these interpretations may be assumed to be strongly related to the level of confidence associated with the simulated value of $K_{aquifer}$. However, it is likely that the degree of contrast between these two parameters is a more significant factor in accurately simulating the observed response than is the actual parameter values used. In spite of this consideration, it can also be stated that the simulated value for $K_{aquifer}$ is assumed to have a fairly high level of confidence since it is based upon transmissivity values calculated from the TW1 pumping test (OMM, 1993a), and since these transmissivity values showed a high level of consistency despite being derived from numerous locations.

Other predictive simulations determined that the rate of tunnel advance had no effect upon the level of impact observed and that it may have been feasible to minimize the number of well interference problems experienced through artificial aquifer recharge using injection wells.

7.4 Model Limitations

The validity of the model described herein is a function of both the degree to which the conceptual model actually describes the physical system simulated, and the degree to which the numerical model accurately represents the conceptual model. The information presented

herein documents the approach that was taken in order to characterize both of these factors. This characterization is inherently limited by the available data and the accuracy of any interpretations made based upon this data.

The most significant limitation in terms of the available data lies in the fact that the vast majority of the data pertaining to the aquifer studied is spatially skewed along the tunnel axis. This is particularly true for parameters such as aquifer transmissivity and storativity, and to a lesser extent, heads and drawdown.

While this may present a significant limitation in terms of the model's ability to accurately represent conditions at locations further removed from the main study area, it is considered to be a much less significant factor in terms of the model's applicability within the study area, where the aquifer has been relatively well characterized.

As described herein, the model was calibrated to both steady state heads and transient heads and flows under stressed conditions. The stressed conditions simulated consisted of both the aquifer's response to the TW1 pumping test and tunnel dewatering. However, since the observed response in terms of drawdown during the TW1 pumping test was generally much lower than the calibration value error level, this data could not be used to quantitatively assess the model calibration. Furthermore, the validity of the calibration to the tunnel dewatering data is tempered by the fact that the simulated response was strongly controlled by a calibration parameter (K_{drain}). Nevertheless, the sum total of these three avenues for calibration (steady state simulation, transient simulation of pumping test, and transient

simulation of tunnel dewatering) provides a reasonable level of confidence when viewed in terms of a 'weight of evidence' approach.

The most significant problem with the transient calibration to drawdown induced by tunnel dewatering was the model's tendency to under-predict drawdown, while over-predicting inflow to the tunnel. From the simulations completed, it is known that some of the error associated with this calibration results from the discretization of time used to simulate the tunnel advance (particularly with respect to flow rates). Clearly, some error also results from the error inherent in the drawdown data. The relatively high modeled recharge values may also be a contributing factor. However, another source of error which may be a factor is the model's use of an equivalent porous medium (EPM) approach. For example, monitoring wells which were located directly along, or in close proximity to, vertical fractures may have shown a stronger response than those located further away from such features (based upon the observed bedding geometry within the tunnel, it is assumed that all wells would have intersected bedding planes). Such effects would not be apparent using the EPM approach (although, arguably, the discrete fracture approach would present another set of untrackable problems).

Lastly, it is noted that the model was determined to be somewhat sensitive to changes in both hydraulic conductivity and recharge, reducing the level of uniqueness of the model solution. However, since the values used for these parameters are believed to be both reasonable and justifiable, and given the level of model calibration obtained, this factor is not considered to present a significant limitation to the use of the model.

8.0 Summary and Conclusions

A numerical groundwater flow model was prepared to simulate the effects of dewatering during the construction of a portion of the West Rideau Collector Sewer tunnel in Nepean, Ontario. The model was constructed through the application of standard groundwater flow modeling techniques using the United States Geological Survey's modular groundwater flow modeling program (MODFLOW).

The modeling was retrospective and consequently benefited from a large database of information, which included actual dewatering rates and groundwater levels measured during the course of tunnel construction. This data allowed the model to be calibrated to the degree that it was found to effectively simulate both steady state and transient (stressed) conditions as actually recorded at the available data locations. This level of calibration was considered to be sufficient to allow the model to be used for predictive purposes.

Key features of the model design included the use of a single layer to represent the aquifer through which the tunnel was constructed, and the simulation of the tunnel itself as a head-dependent (drain) boundary which advances with time. The aquifer was defined as a single hydrostratigraphic unit comprising the dolostone of the Oxford Formation and an overlying glacial till sequence. The construction of a 1,400 metre length of tunnel through this aquifer was simulated through the progressive addition of 200 metre tunnel segments through seven stress periods.

During model calibration, the tunnel advance was also simulated with tunnel segments of 100 metres and 700 metres, using fourteen and two stress periods, respectively. These variations were found to have only a minor effect on the simulated aquifer response in terms of drawdown, but had a more significant effect in terms of the predicted rate of groundwater inflow to the tunnel. However, even using only two stress periods, the predicted rate of inflow still provided a reasonable approximation of the flow rates actually recorded.

Consequently, it was concluded that the way in which the tunnel advance is represented in terms of the discretization of time is not a significant factor in simulating the overall impact to the aquifer from tunnel dewatering. This observation reflects the fact that the rate of tunnel advance is sufficiently slow to allow the aquifer's response to become asymptotic (approaching a steady state response to the applied stress) on a shorter time scale than both the rate of tunnel mining and the subsequent installation of an impermeable liner. For this same reason, it was concluded that it is not necessary for the model to specifically account for groundwater inflows at the tunnel face, which has been a focus of modeling work completed by other investigators. Stated another way, it is not important to quantify inflows at the tunnel face when evaluating tunnel dewatering impacts from what has been termed herein as a 'hydrogeological' perspective (the impact to the overall flow system). It is however recognized that the rate of groundwater inflow at the tunnel face can be important when evaluating tunnel dewatering as an engineering problem. In this latter case, it is noted that the method implemented in this study could also be adapted to quantify inflows at the tunnel

face through applying smaller discretizations both spatially and temporally to the leading edge of the simulated tunnel.

In terms of the model's representation of grouting efforts that were completed to reduce the rate of groundwater inflow to the tunnel, it was assumed that the effectiveness of this grouting program could be directly related to the contrast between the hydraulic conductivity of the aquifer ($K_{aquifer}$) and the hydraulic conductivity of the grouted rock immediately surrounding the tunnel (K_{drain}). With this in mind, the calibrated model used a value for K_{drain} which was 17 times lower than that of $K_{aquifer}$. The results of predictive simulations completed using the calibrated model showed that increasing this contrast to a factor of 40 times may have been sufficient to effectively eliminate the occurrence of well interference problems. Alternatively, it was shown that the tunnel's impact would have been substantially greater had no grouting efforts been completed (i.e. $K_{drain} = K_{aquifer}$).

The results of other predictive simulations showed that the rate of tunnel advance had no effect upon the level of impact observed and that it may have been feasible to minimize the number of well interference problems experienced through artificial aquifer recharge using injection wells.

The most significant limitation to the use of this model stems from the means through which the model was calibrated to stressed conditions. This involved a qualitative calibration to the observed aquifer response to a pumping test, along with a more quantitative calibration to the observed response to tunnel dewatering. Calibration to this latter data set must be considered

less definitive since the calibration was strongly influenced by a calibrated parameter (K_{drain}). Nevertheless, the sum total of these two avenues for calibration, along with the calibration to steady state data, was considered to provide a reasonable level of confidence when viewed in terms of a 'weight of evidence' approach. This level of confidence would be increased through the simulation of another aquifer stress which was not dependent upon a calibration parameter and produced a measured response greater than the calibration value error level.

References

Anagnostou, G. 1995. **The Influence of Tunnel Excavation on the Hydraulic Head.** *International Journal for Numerical and Analytical Methods in Geomechanics*, Vol. 19, pp. 725-746.

Anderson, M.P. and Woessner, W.W. 1992. **Applied Groundwater Modeling, Simulation of Flow and Advective Transport**. Academic Press Inc., San Diego, California.

Bélanger, J. R., Howard, M., Moore, A. and Prégent, A. 1977. **Bedrock Geology and Geotechnical Characteristics of Rock Formations of the National Capital Region, Ontario-Québec**, Digital Maps. Geological Survey of Canada Open File no. 2884.

CCME, 1996. **Derivation of Recharge Factor for Recharge Water in Groundwater.** *in* A Protocol for the Derivation of Environmental and Human Health Soil Quality Guidelines. Canadian Council of Ministers of the Environment.

CHS, 1984. **Rideau Waterway, Small-Craft Chart – Ottawa to Smiths Falls.** Ministry of Fisheries and Oceans Canada, Canadian Hydrographic Service.

Driscoll, F.G. 1986. **Groundwater and Wells**. Johnson Division, St. Paul, Minnesota.

Dupuit, J. 1863. **Etudes théoriques et pratiques sur le mouvement des eaux dans les canaux découverts et a travers les terrains perméables**. Dunod, Paris.

Eberts, S.M. and Bair, E.S. 1990. **Simulated Effects of Quarry Dewatering Near a Municipal Well Field.** *Ground Water*, Vol. 28, pp. 37-47.

Forchheimer, P. 1930. **Hydraulik**. Teubner Verlagsgesellschaft, Stuttgart.

Freeze, R.A., and Cherry, J.A. 1979. **Groundwater**. Prentice-Hall Inc., Englewood Cliffs, N.J.

Gale, J.E. 1982. **Assessing the Permeability Characteristics of Fractured Rock**, Geological Society of America Spec. Paper 189, pp. 163-181.

Goodman, R.E., Moye, D.G., Van Schalwyk, A. and Javandel, I. 1965. **Groundwater Inflows During Tunnel Driving**. *Engineering Geology*, Vol. 2, pp. 39-56.

Hantush, M.S. and Jacob, C.E. 1955. **Non-Steady Radial Flow in an Infinite Leaky Aquifer**. Transactions of the American Geophysical Union, Vol. 36, pp. 95-100.

Hill, M.C. 1995. **Preconditioned Conjugate-Gradient 2 (Pcg2), A Computer Program For Solving Ground-Water Flow Equations (Version 2.1).** Electronic Manual for MODFLOW Packages, Environmental Simulations Inc.

McDonald, M.G. and Harbaugh, A.W. 1988. **A Modular Three-Dimensional Finite-Difference Groundwater Flow Model**. *Techniques of Water-Resources Investigations* 06-A1, United States Geological Survey.

McKee, J.A., MacGillis, S.C., and Wilson, S.R., 1994. **Hydrogeological Considerations and Groundwater Control for the West Rideau Collector Sewer-Phase III**. *12th Annual Tunneling Congress, Tunneling Association of Canada*, Vancouver, October 1994.

Oliver Mangione McCalla and Associaes Ltd. (OMM) 1993a. **Planning and Design Stage Report on Hydrogeological Studies for the West Rideau Collector Sewer (Phase III).** Unpublished report.

Oliver Mangione McCalla and Associaes Ltd. (OMM) 1993b. **Hydrogeological Investigation, West Rideau Collector Sewer - Phase III, Factual Report**. Unpublished report.

Richard, S.H. 1976. **Surficial Geology, Ottawa, Ontario-Quebec**; Geological Survey of Canada, Map 1506A, Scale 1:50,000.

RVCA, 1980. **Jock River Flood Plain Mapping**, Sheet 1 – Sheet 4. Rideau Valley Conservation Authority.

Scweiger, H.F., Resch, M.M., Haas, W., Faust, P. and Pottler, R., 1993. **Influence of Tunneling on the Groundwater Level in an Environmentally Sensitive Area**. Eurock '93, Ribeiro e Sousa & Grossman (eds), Balkema, Rotterdam.

Toran, L. and Bradbury, K.R. 1988. **Ground-Water Flow Model of Drawdown and Recovery Near an Underground Mine**. *Ground Water*, Vol. 26, pp.724-733.

Zheng, C. 1990. **MT3D, a Modular Three Dimensional Transport Model for Simulation of Advection, Dispersion and Chemical Reactions of Contaminants in Groundwater Systems**. S.S. Papadopulos & Assoc., Rockville, Maryland.

Appendix A

Aquifer Properties

Table A1
Transmissivity and Storativity Values from Design Stage Pumping Tests (OMM, 1993)

TW1 Pumping Test

Location	Radius (m)	Analytical Method	Transmissivity (m^2/s)	Storativity
92-104s	85	Hantush	1.1E-03	4.2E-04
89-3s	140	Hantush	1.2E-03	2.1E-04
92-103s	150	Hantush	1.2E-03	2.9E-03
92-102s	320	Theis	1.4E-03	2.5E-03
92-108s	625	Theis	1.1E-03	5.5E-04
92-104d	85	Hantush	1.5E-03	1.1E-04
89-2s	235	Cooper-Jacob	1.2E-03	7.5E-04
89-4s	445	Theis	1.2E-03	5.5E-04
89-4d	445	Cooper-Jacob	1.9E-03	1.7E-03
92-108d	625	Theis	1.2E-03	8.6E-04
		Arithmetic Mean	**1.3E-03**	**1.1E-03**

TW2 Pumping Test

Location	Radius (m)	Analytical Method	Transmissivity (m^2/s)	Storativity
89-7d	175	Theis	9.5E-04	5.2E-07
89-6d	530	Theis	5.2E-04	4.2E-04
89-5s	895	Theis	1.5E-04	3.4E-04
89-5d	895	Theis	1.8E-03	2.6E-04
TW2	0	Cooper-Jacob	9.9E-05	
TW2 (rec)	0	Theis recovery	4.2E-04	
92-113	65	Theis	2.5E-04	3.1E-03
89-7s	175	Theis	7.9E-04	2.2E-06
92-114	245	Theis	3.5E-04	5.4E-04
92-111s	260	Theis	6.4E-04	2.8E-04
92-111d	260	Theis	6.4E-04	1.1E-04
OMM5d	275	Theis	5.3E-04	9.4E-05
92-115	320	Theis	4.0E-04	3.0E-04
89-6s	530	Theis	6.6E-04	3.0E-04
		Arithmetic Mean	**9.5E-04**	**8.9E-04**

Table A2
Layer Top Elevations

Location	X	Y	Top of Till	Top of Rock	Top of Layer 1
E1	1770	5460		77.5	77.5
E2	1500	5510	79.4	78.8	79.4
E3	1600	5550	79.6	76.2	79.6
E4	1900	5850		71.8	71.8
E5	1920	5700	83.9	72.6	83.9
E6	1630	5900	79.8	64.6	79.8
E7	1800	6100	72.2	66.7	72.2
E8	1770	5800	83.4	73.3	83.4
E9	3800	5850		68.9	68.9
E10	3700	5675		82.0	82.0
E11	3025	5790	79.4	77.6	79.4
E12	2750	6250	78.8	77.9	78.8
E13	2585	6350		75.5	75.5
E14	1800	6200	67.8	60.8	67.8
E15	1950	6000	71.2	69.9	71.2
E16	1750	6400		56.1	56.1
C1	1600	4200		75.3	75.3
C2	1500	4950		75.5	75.5
C3	1380	3110		81.7	81.7
C4	1380	3050		83.8	83.8
C5	1410	3300		84.0	84.0
C6	1480	3510		79.2	79.2
C7	1300	3620		73.7	73.7
C8	1430	3580		80.5	80.5
C9	1400	3700		79.2	79.2
C10	1320	3380		81.4	81.4
C11	1340	5000		79.2	79.2
C12	1170	4650	83.9	80.9	83.9
C13	1200	4780	84.5	79.3	84.5
C14	1400	3050		78.9	78.9
C15	1620	4750		77.4	77.4
C16	1600	4650		76.5	76.5
A1	2450	3800		75.4	75.4
A2	2220	4000		74.2	74.2
A3	2390	4150		75.4	75.4
A4	2350	4225	82.3	75.9	82.3
A5	2220	4060		77.8	77.8
A6	2300	4425	87.4	75.8	87.4
A7	2480	3900		75.6	75.6
A8	2470	4070	76.5	75.3	76.5
A9	2270	4400	84.1	78.9	84.1
A10	2570	4000		75.7	75.7

Location	X	Y	Top of Till	Top of Rock	Top of Layer 1
A11	2330	3800		75.9	75.9
A12	2300	3780		77.2	77.2
A13	2480	4550		75.4	75.4
A14	2460	4570		76.2	76.2
A15	2230	3800		77.5	77.5
A16	2430	3960		72.3	72.3
A18	2220	3720		76.9	76.9
A19	2330	4000		76.2	76.2
A20	2550	3780	80.3	75.1	80.3
A21	2470	4250		74.6	74.6
A22	2510	4600		77.1	77.1
A23	2490	4500	83.4	76.1	83.4
A24	2510	4580		77.1	77.1
A26	2580	3700	80.3	76.0	80.3
B1	5550	850	84.4	83.2	84.4
89-1*	2010	5040	84.5	83.3	84.5
92-102*	2226	4992	83.8	83.3	83.8
92-104*	2636	5020	84.7	81.8	84.7
92-108*	3193	5040	84.8	82.1	84.8
92-111*	3963	5050	82.2	81.9	82.2
92-113*	4276	5020	75.7		75.7
94-1*	4616	5040	74.4	69.9	74.4
94-202*	5155	5051	73	71.8	73
OMM1*	1820	5328		77.6	77.6
OMM2*	2037	5335		78.3	78.3
OMM3*	2112	4842	82.8	77.8	82.8
				Average	~~80.0~~ 78.1

Source: * OMM, 1993b
all others from MOE water well records

Appendix B

Calibration Values

Table B1

Pumping rates - MacFarlane Shaft

(rates of groundwater inflow over entire tunnel length)

Stress Period 1

date	Q (gpm)
09-May-94	26
10-May-94	40
11-May-94	60
12-May-94	60
13-May-94	62
14-May-94	62
15-May-94	62
16-May-94	76
17-May-94	75
18-May-94	86
19-May-94	85
20-May-94	87
21-May-94	87
22-May-94	87
23-May-94	87
24-May-94	100
25-May-94	101
26-May-94	133
27-May-94	145
28-May-94	145
29-May-94	145
30-May-94	154
31-May-94	75
01-Jun-94	73
02-Jun-94	88
03-Jun-94	195
Q (gpm)	92.16385
Q (l/min)	419.3
Q (m^3/day)	603.792

Stress Period 2

date	Q (gpm)
04-Jun-94	195
05-Jun-94	195
06-Jun-94	175
07-Jun-94	130
08-Jun-94	130
09-Jun-94	130
10-Jun-94	130
11-Jun-94	130
12-Jun-94	130
13-Jun-94	130
14-Jun-94	145
15-Jun-94	106
16-Jun-94	106
17-Jun-94	106
18-Jun-94	106
19-Jun-94	106
20-Jun-94	106
21-Jun-94	106
22-Jun-94	106
23-Jun-94	106
24-Jun-94	150
25-Jun-94	150
26-Jun-94	150
27-Jun-94	105
28-Jun-94	100
29-Jun-94	113
30-Jun-94	108
01-Jul-94	108
02-Jul-94	108
03-Jul-94	108
04-Jul-94	108
05-Jul-94	193
06-Jul-94	193
07-Jul-94	193
08-Jul-94	169
Q (gpm)	132.2857
Q (l/min)	601.9
Q (m^3/day)	866.736
cum. avg.	
gpm	115
l/min	523

Stress Period 3

date	Q (gpm)
09-Jul-94	175
10-Jul-94	175
11-Jul-94	180
12-Jul-94	180
13-Jul-94	169
13-Jul-94	169
14-Jul-94	159
14-Jul-94	159
18-Jul-94	193
19-Jul-94	160
20-Jul-94	176
21-Jul-94	176
22-Jul-94	180
25-Jul-94	182
26-Jul-94	183
27-Jul-94	183
Q (gpm)	175.0625
Q (l/min)	796.5344
Q (m^3/day)	1147.01
cum. avg.	
gpm	131
l/min	596

Stress Period 4

date	Q (gpm)
28-Jul-94	184
29-Jul-94	184
30-Jul-94	187
31-Jul-94	187
1-Aug-94	188
2-Aug-94	183
3-Aug-94	188
4-Aug-94	201
5-Aug-94	203
6-Aug-94	201
7-Aug-94	201
8-Aug-94	199
9-Aug-94	201
10-Aug-94	199
11-Aug-94	197
Q (gpm)	193.5333
Q (l/min)	880.5767
Q (m^3/day)	1268.03
cum. avg.	
gpm	141
l/min	642

Stress Period 5

date	Q (gpm)
12-Aug-94	200
13-Aug-94	208
14-Aug-94	207
15-Aug-94	199
16-Aug-94	191
17-Aug-94	194
18-Aug-94	195
19-Aug-94	193
20-Aug-94	190
21-Aug-94	190
22-Aug-94	190
23-Aug-94	187
24-Aug-94	189
25-Aug-94	190
26-Aug-94	190
27-Aug-94	202
28-Aug-94	205
29-Aug-94	211
30-Aug-94	208
31-Aug-94	208
1-Sep-94	206
2-Sep-94	209
3-Sep-94	209
4-Sep-94	209
5-Sep-94	209
6-Sep-94	208
7-Sep-94	207
Q (gpm)	200.1481
Q (l/min)	910.6741
Q (m^3/day)	1311.371
cum. avg.	
gpm	152
l/min	692

Stress Period 6

date	Q (gpm)
8-Sep-94	207
9-Sep-94	204
10-Sep-94	209
11-Sep-94	209
12-Sep-94	212
13-Sep-94	205
14-Sep-94	208
15-Sep-94	214
16-Sep-94	226
17-Sep-94	225
18-Sep-94	213
19-Sep-94	233
20-Sep-94	230
21-Sep-94	227
22-Sep-94	226
23-Sep-94	223
24-Sep-94	222
25-Sep-94	229
26-Sep-94	226
Q (gpm)	218.4211
Q (l/min)	993.8158
Q (m^3/day)	1431.095
cum. avg.	
gpm	163
l/min	742

Stress Period 7

date	Q (gpm)
27-Sep-94	228
28-Sep-94	245
29-Sep-94	245
30-Sep-94	250
1-Oct-94	255
2-Oct-94	255
3-Oct-94	248
4-Oct-94	226
5-Oct-94	239
6-Oct-94	225
7-Oct-94	244
8-Oct-94	235
9-Oct-94	238
10-Oct-94	237
11-Oct-94	235
12-Oct-94	240
13-Oct-94	240
14-Oct-94	226
15-Oct-94	251
16-Oct-94	249
17-Oct-94	248
18-Oct-94	241
19-Oct-94	246
20-Oct-94	238
21-Oct-94	240
22-Oct-94	220
23-Oct-94	204
24-Oct-94	214
25-Oct-94	233
26-Oct-94	214
27-Oct-94	240
28-Oct-94	232
29-Oct-94	238
30-Oct-94	234
31-Oct-94	231
Q (gpm)	236.6857
Q (l/min)	1076.92
Q (m^3/day)	1550.765
cum. avg.	
gpm	178
l/min	810

Table B2
Calibration Values for Transient Simulations

Target Location	Time (Days)	Observed Drawdown	Computed Drawdown	Residual
omm3	25	3.00	2.31	0.69
	59	3.10	3.55	-0.45
	80	3.20	3.92	-0.72
	95	3.55	3.95	-0.40
	117	3.90	3.97	-0.07
	140	4.30	3.99	0.31
	176	4.60	4.01	0.59
omm4	25	3.00	1.60	1.40
	59	3.50	3.38	0.12
	80	3.65	4.01	-0.36
	95	4.03	4.03	0.00
	117	4.40	4.05	0.35
	140	4.45	4.06	0.39
	176	4.70	4.08	0.62
92-102	25	4.40	1.83	2.57
	59	4.65	4.10	0.55
	80	4.95	4.67	0.28
	95	5.05	4.69	0.36
	117	5.70	4.71	0.99
	140	6.15	4.72	1.43
	176	6.50	4.74	1.76
92-101	25	4.00	3.15	0.85
	59	3.40	3.99	-0.59
	80	3.80	4.24	-0.44
	95	3.95	4.26	-0.31
	117	4.55	4.28	0.27
	140	4.95	4.30	0.65
	176	5.35	4.32	1.03
omm1	25	2.80	1.62	1.18
	59	2.20	2.27	-0.07
	80	2.70	2.49	0.21
	95	3.08	2.51	0.57
	117	3.45	2.53	0.92
	140	3.90	2.55	1.35
	176	4.25	2.57	1.68
omm2	25	2.60	1.96	0.64
	59	2.30	2.86	-0.56
	80	2.75	3.16	-0.41
	95	2.90	3.18	-0.28
	117	3.55	3.19	0.36
	140	3.90	3.21	0.69
	176	4.25	3.22	1.03
TW1	25	0.50	0.15	0.35
	59	0.65	0.33	0.32
	80	0.80	1.03	-0.23
	95	0.85	1.18	-0.33
	117	0.95	1.20	-0.25
	140	1.00	1.21	-0.21
	176	1.20	1.22	-0.02
85-7	25	3.75	1.58	2.17
	59	2.50	2.22	0.28
	80	3.50	2.42	1.08
	95	3.45	2.45	1.00
	117	4.25	2.48	1.77
	140	5.25	2.50	2.75
	176	6.25	2.52	3.73
92-104	95	1.35	0.54	0.81
	117	1.65	0.67	0.98
	140	2.00	0.73	1.27
	176	2.35	0.76	1.59
r89-3	95	0.70	0.64	0.06
	117	1.23	1.14	0.09
	140	1.76	1.38	0.38
	176	2.30	1.51	0.79
omm7	95	0.35	0.26	0.09
	117	5.95	1.62	4.33
	140	6.00	2.60	3.40
	176	3.70	3.05	0.65
r89-4	95	0.15	0.20	-0.05
	117	1.58	0.97	0.61
	140	3.00	2.84	0.16
	176	3.40	3.58	-0.18
gb1	95	0.20	0.20	0.00
	117	1.10	0.66	0.44
	140	1.55	1.53	0.02
	176	1.85	2.31	-0.46
r89-5	95	0.43	0.13	0.30
	117	1.54	0.44	1.10
	140	1.90	1.18	0.72
	176	2.63	2.58	0.05
omm8	176	1.30	1.79	-0.49
r89-6	176	1.30	1.25	0.05

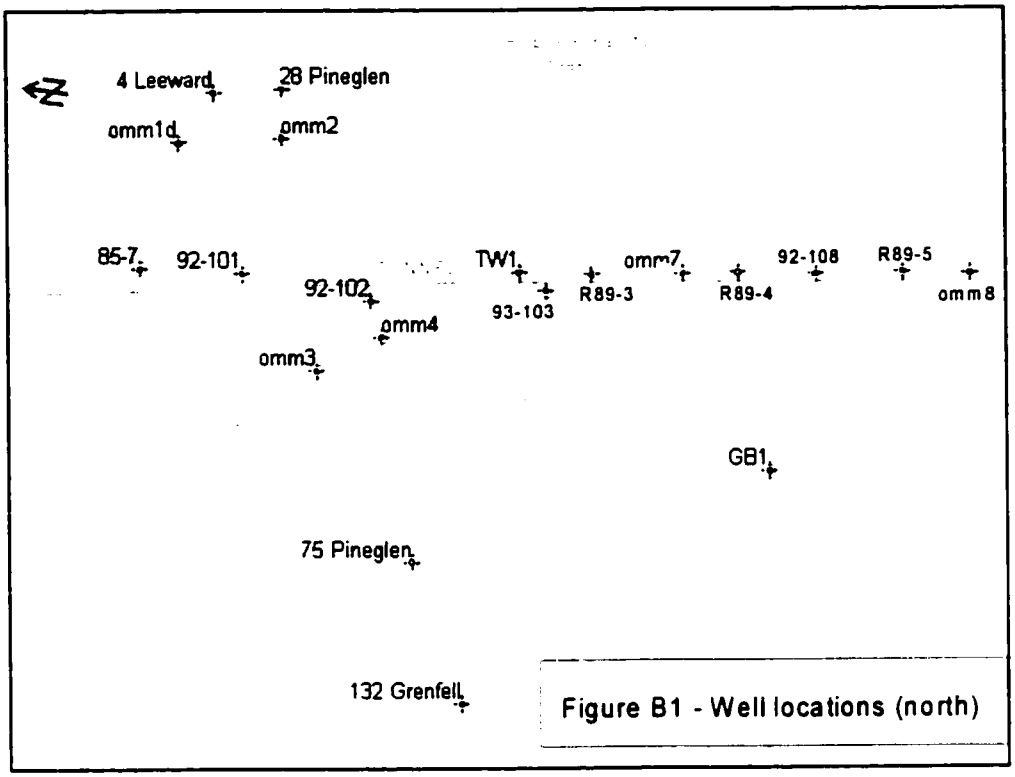

Figure B1 - Well locations (north)

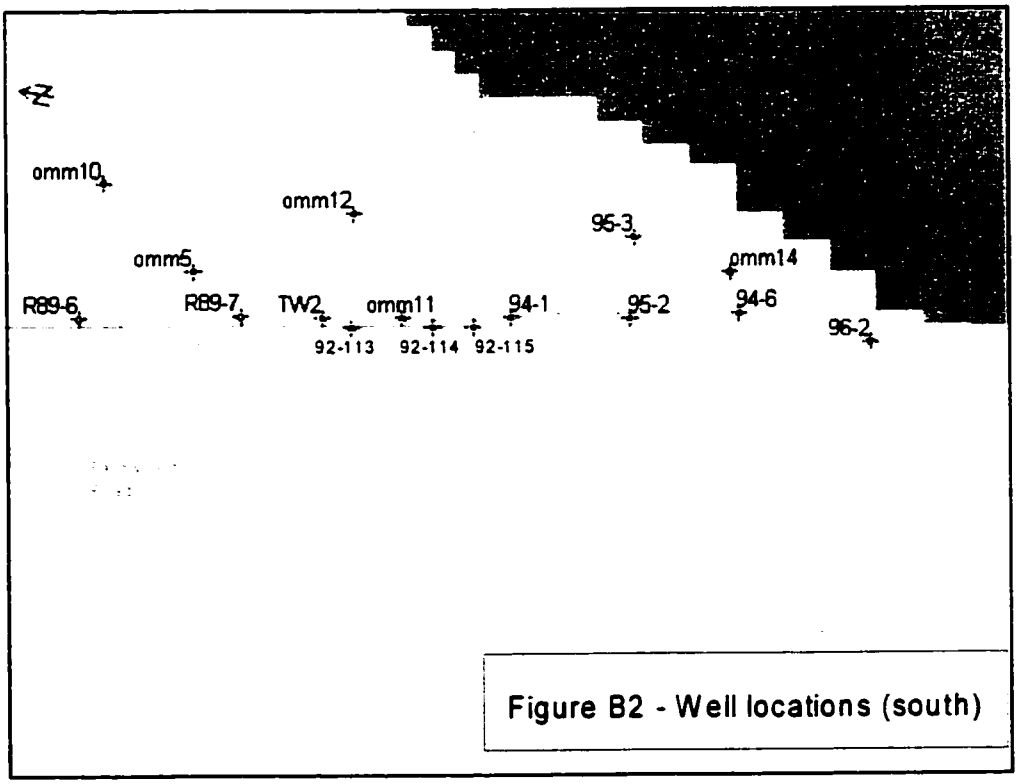

Figure B2 - Well locations (south)